A Study on the Analysis of Treadmill Perturbation Data for the Design of Active Ankle Foot Orthosis to Prevent Falls and Gait Rehabilitation

by

Sambarta Ray

A Thesis Presented in Partial Fulfillment
of the Requirements for the Degree
Master of Science

Approved July 2020 by the
Graduate Supervisory Committee:

Gautam Dasarathy, Co-Chair
Claire Honeycutt, Co-Chair
Sangram Redkar
Suren Jayasuriya

ARIZONA STATE UNIVERSITY

August 2020

ABSTRACT

According to the Center for Disease Control and Prevention report around 29,668 United States residents aged greater than 65 years had died as a result of a fall in 2016. Other injuries like wrist fractures, hip fractures, and head injuries occur as a result of a fall. Certain groups of people are more prone to experience falls than others, one of which being individuals with stroke. The two most common issues with individuals with strokes are ankle weakness and foot drop, both of which contribute to falls. To mitigate this issue, the most popular clinical remedy given to these users is thermoplastic Ankle Foot Orthosis. These AFO's help improving gait velocity, stride length, and cadence. However, studies have shown that a continuous restraint on the ankle harms the compensatory stepping response and forward propulsion. It has been shown in previous studies that compensatory stepping and forward propulsion are crucial for the user's ability to recover from postural perturbations. Hence, there is a need for active devices that can supply a plantarflexion during the push-off and dorsiflexion during the swing phase of gait. Although advancements in the orthotic research have shown major improvements in supporting the ankle joint for rehabilitation, there is a lack of available active devices that can help impaired users in daily activities. In this study, the primary focus is to build an unobtrusive, cost-effective, and easy to wear active device for gait rehabilitation and fall prevention in individuals who are at risk. The device will be using a double-acting cylinder that can be easily incorporated into the user's footwear using a novel custom-designed powered ankle brace. The device will use Inertial Measurement Units to measure kinematic parameters of the lower body and a custom control algorithm to actuate the device based on the measurements. The study can be used to advance the field of gait assistance, rehabilitation, and potentially fall prevention of individuals with lower-limb impairments through the use of Active Ankle Foot Orthosis.

DEDICATION

I would like to dedicate this to my Family and Friends who have continuously motivated me and inspired me to reach greater heights in life.

ACKNOWLEDGMENTS

First and foremost I would like to thank Dr. Claire Honeycutt for offering me the opportunity of pursuing my Master's degree and being able to work on this interesting project. I would also like to thank Dr. Sangram Redkar for allowing us to build the device in his lab and providing us with essential feedback. Furthermore, I would like to thank my committee members Dr. Gautam Dasarathy and Dr. Suren Jayasuriya for their support. I would like to thank Jason Olson for his help in designing the ankle brace for the orthosis and for helping me assemble and test the device. I would also like to thank all my lab members who have given valuable suggestions and feedback for the study.

Lastly, I am grateful to the BRAIN Center for supporting the project and to Arizona State University for providing the infrastructure to design, build, and test our device.

TABLE OF CONTENTS

CHAPTER Page

LIST OF TABLES

LIST OF FIGURES

Figure Page

Chapter 1

DESIGN OF ACTIVE ANKLE FOOT ORTHOSIS

1.1 Introduction

Certain groups of people are more susceptible to experience falls than others, one of which being stroke survivors. Although the risk of stroke increases with age, a stroke can occur at any age, and the most common type of stroke inhibits blood flow to the brain cdc (2020). The brain is responsible for sending motor signals to muscles through the nervous system required for muscle movement. After a stroke, these signals get affected and can delay muscle, both kinetic and kinematic responses to perturbation Weerdesteyn *et al.* (2008). Falls are the common complaints that individuals with such impairment have during or after their rehabilitation phase. Statistics on after stroke falls Batchelor *et al.* (2012) reveal that 14%-65% patients fall during hospitalization and between 37%-73% fall during the first 6 months of discharge from hospital. According to the CDC article by Burns and Kakara (2018), it is shown that in 2016 around 29,668 US residents aged $\geq$ 65 years had died as a result of a fall. Severe injuries like wrist fractures, hip fracture, and head injury occur due to falling as shown in the studies of Ramnemark *et al.* (1998), Dennis *et al.* (2002) and Pouwels *et al.* (2009). In the studies by Jørgensen *et al.* (2002) and Herndon *et al.* (1997), it is shown that individuals with stroke are at high risk of falling and is the most common medical complication after stroke. It's shown in the study by Yarkony and Sahgal (1987) that around 67% of individuals with stroke suffer from ankle weakness and in the study by Wade *et al.* (1985), it's shown that approximately 20% of individuals with stroke suffer from foot drop issues.

1.1.1 Requirement for an Active Ankle-Foot Orthosis

Orthotic devices are primarily used by people with partial or complete loss of muscle activity (paresis) in their extremities. This loss of muscle activity leads to motor-issues such as drop foot (i.e. inability to lift the impaired foot during the swing phase of gait) or spasticity (i.e. stiffness and tightening of muscles) of lower limb muscles. These issues lead to the loss of postural control Geurts *et al.* (2005) increasing the risk of falls among those affected. Falls most commonly result in soft tissue damage and can lead to fractures or death in severe cases. Along with physical injuries, falls can also cause psychological trauma, associated with fear of falling that can lead to deficits in gait and balance, reduced physical activities, and deconditioning as found in Hatem *et al.* (2016). The most commonly prescribed clinical remedy provided to tackle drop foot issue and improper gait is passive thermoplastic Ankle Foot Orthosis (AFO), which are designed to lock the paretic ankle joint at a certain angle, facilitate foot clearance during swing phase, ankle stability during stance phase and heel strike as studied in Taborri *et al.* (2016) and Kluding *et al.* (2013). While there are reported improvements of gait velocity, stride length, and cadence(steps/min) as shown in the study by Simons *et al.* (2009), studies by Nevisipour (2019) show that continual constraints in the ankle joint adversely affect the compensatory stepping response, forward propulsion and proprioceptive sensory information. Studies from Mcilroy and Maki (1993) and Jensen *et al.* (2001) show that for the subject to prevent falls from postural perturbations, the compensatory stepping response is crucial. Therefore continually restricting the ankle movement might adversely affect the user's ability to recover from sudden perturbations.

The study by Alam *et al.* (2014) highlights that the primary cause of musculoskeletal weakness is the weakness in plantar flexor and dorsiflexor of the ankle. The weak-

ness in plantar flexors causes a reduced *forward propulsion* that would result in weak push-off during the Pre-swing (push-off) of the stance phase. The weakness in the dorsiflexors would result in an insufficient clearance of the toe during the Mid Swing of the swing phase and would reduce the step length, force toe dragging, lower walking speeds and increase the overall chances of tripping. The various phases of gait cycles are referred from the study in Taborri *et al.* (2016). As mentioned in the study by Alam *et al.* (2014), two of the major complications of the above mentioned weakness are the *foot slap* which is the uncontrolled and rapid strike of foot and *toe drag* which is the dragging of the forefoot due to insufficient clearance during Mid Swing. Therefore, there is a need for an AAFO that can deliver powered push off for a stronger plantar flexion, locking of the ankle joint during the swing phase to prevent dragging of the paretic foot and a stable foot strike.

1.1.2 Study of Existing Devices

Advancements in orthotics research have provided AFO devices that have shown improvement in supporting the ankle joint as rehabilitation devices for individuals with lower body impairments. There are primarily 3 different types of AFOs that are used for addressing the issue of drop foot and lower limb impairments - passive AFO, semi-active AFO, and active AFO. The passive AFO is the most commonly prescribed AFO and usually consists of a thermoplastic element that locks the ankle joint at a certain angle which is effective in foot clearance since it reduces the chances of the foot striking an obstacle during Mid Swing. However, the restriction in the ankle movement prevents the ankle from generating strong push-off torque and normal ankle movements. The semi-active AFO usually varies the flexibility of the ankle joint by using an externally controlled damper system. In the studies by Yamamoto

et al. (1997), specialized joints using stiffness control elements, flexion stops, and a one-way friction clutch are used to control the ankle movement in the sagittal plane. The Active AFOs usually consist of an external power source, sensors for detecting movements in the essential body parts, the control algorithm for articulating the ankle joint in a dynamic way. The study by Alam *et al.* (2014) highlights some of the common control elements used by different ankle-foot orthotics.

- **Spring:** In the study by Palmer (2002), linear torsional springs are used for controlling the plantar flexion. the spring would get loaded during the loading response of the stance phase and would generate a forward propulsion during the pre-swing (push-off) phase of the gait cycles. These elements are not very effective in dorsiflexion which in some cases reduce normal movement of the ankle.

- **Series Elastic Actuator:** The paper by Hwang *et al.* (2006) shows the use of the Series Elastic Actuator (SEA) for controlling the ankle actuation. In this type of actuator an elastic element, most commonly a spring is attached in series to a DC motor. An external processing unit is then used for deflecting the elastic element to generate output force on the ankle joint. In these types of design the heavier element like the motor and the springs are usually attached to the leg of the users which tends to hinder the user comfort and wearability of the device. Other SEA device such as the robotic tendon AFO Boehler *et al.* (2008) utilizes a similar configuration of a DC motor in series with a custom-built lead screw and a spring. The device has shown improvement in providing push off assistance to the user, although it sacrifices some level of user comfort with the chosen force and fastening method.

- **Passive Pneumatic Element:** The use of passive pneumatic elements has

been studied by Kawamura *et al.* (2002). The use of these elements benefit adjustability of ankle joint stiffness and initial ankle angle that are important for controlling the body alignment for walking.

- **Artificial Pneumatic Muscle:** Pneumatic actuators has been shown to be an effective supplementation of the soleus and the gastrocnemious muscles. The designs by Ferris *et al.* (2005) and Ferris *et al.* (2006) utilized McKibben pneumatic muscles to develop tethered powered ankle foot orthosis. These ankle foot orthosis have shown to be effective for both plant flexion and dorsi flexion of the ankle joint. Their effectiveness in helping in the ankle flexion in both direction motivates the design of the device in this thesis.

1.1.3 Objectives and Hypothesis

The above section highlights the extensive studies that have been conducted to address the issues with drop foot and paretic limbs. Some of the devices which are capable of addressing the issues of weaker plantarflexion during the push-off phase and an insufficient foot clearance during mid-swing phase of the gait cycle has been described in the above section. The need for an active ankle-foot orthosis is highlighted by studies conducted by Nevisipour (2019). However, there is a lack of commercially available Active Devices that can help impaired users in daily activities. Almost all the devices mentioned above are useful in laboratory conditions and does not address the need for rehabilitating the gait for the ease of performing daily activities. Some of the key negative factors of these devices as highlighted by Alam *et al.* (2014) are tethered powered systems, bulky contraptions that increase the overall weight that is carried by the ankle, adaptability of the devices in dynamic conditions. Most of the devices utilize some sort of angle measuring sensors, foot pressure sensors, and

highly expensive and laboratory-controlled motion capture systems for detecting the conditions of actuation. Although these techniques are useful in a very controlled environment they become either unreliable or impractical in daily use of the devices by the users. There is a need for analyzing the data collected through such laboratory instruments to determine a more mobile method of detecting falls and recoveries resulting from perturbations.

The **first objective** of this thesis is to design an unobtrusive, cost-effective, easy to wear, AAFO which is capable of housing a remote power unit and can be easily incorporated into the user's daily footwear. The device will be designed by double-acting pneumatic cylinders for actuation, Inertial Measurement Units (IMUs) for tracking the kinematic leg motion, and a novel custom printed shoe attachment system. It is **hypothesized** is that such a device will be able to sense the various phases of gait cycles from the attached sensors and will be able to generate a stronger ground reaction force during push-off and sufficient toe clearance by locking the ankle joint only during the swing phase of the gait cycle. The **second objective** of this thesis is to analyze kinematic parameters of users during treadmill-based perturbations to determine effective sensor placement and potential parametric thresholds that would distinguish stepping responses between falls and recoveries. Additionally, it can also potentially detect whether an actuation is required in the stepping of the base leg such that the overall device only actuates when a stepping response is detected to be a potential fall by the sensors. It is **hypothesized** that out of the multiple lower body kinematic parameters that can be measured, there exists a subset of those features that can be used to determine whether a sudden perturbation during stance phase would result in a fall or recovery and whether the first actuated response is sufficient to aid in the recovery. The *expected outcome* of the study is the design an active ankle-foot device that can potentially aid in gait rehabilitation and a set of kinematic

parameters that can be measured using IMU sensors for the detection of falls.

In the first chapter of the thesis, the overall design, mechanical components, electronic components, and the control algorithm that are utilized in the design of the active ankle-foot orthosis is described. In the second chapter of the thesis, the data analysis of treadmill perturbation data to determine the most effective kinematic parameters is described.

1.2 System Design

1.2.1 Design of the Mechanical System

The primary contributor to the kinetic energy and the speed of the stepping leg is forward propulsion force which is generated by the plantarflexor muscles as described in Francis *et al.* (2013). The AAFO's design accomplishes this by taking a mechanical approach to supplement the Soleus and gastrocnemius muscles in a controlled manner while allowing for the maximum range of motion and comfort of the user. The design offers reasonable accommodation to a variety of users with respect to shoe size and weight and can be quickly adjusted such that it does not reduce the range of motion of the ankle. Adjustments are made either through replacement of the lever arm, as well as tightening or loosening of the turnbuckle connecting rods. These adjustments allow the AAFO to operate at up to approximately 25 degrees of Dorsiflexion, and up to approximately 70 degrees of plantarflexion. The connecting rods use swivel-ball ends which allow some degree of foot rotation as well as inversion and eversion of the foot. The dorsiflexion represented by Angle a and plantarflexion represented Angle b can be seen in figure1.1. The AAFO's uses 8 self-tapping screws to secure it to a running or walking shoe and can be adapted to fit a range of shoe sizes and styles,

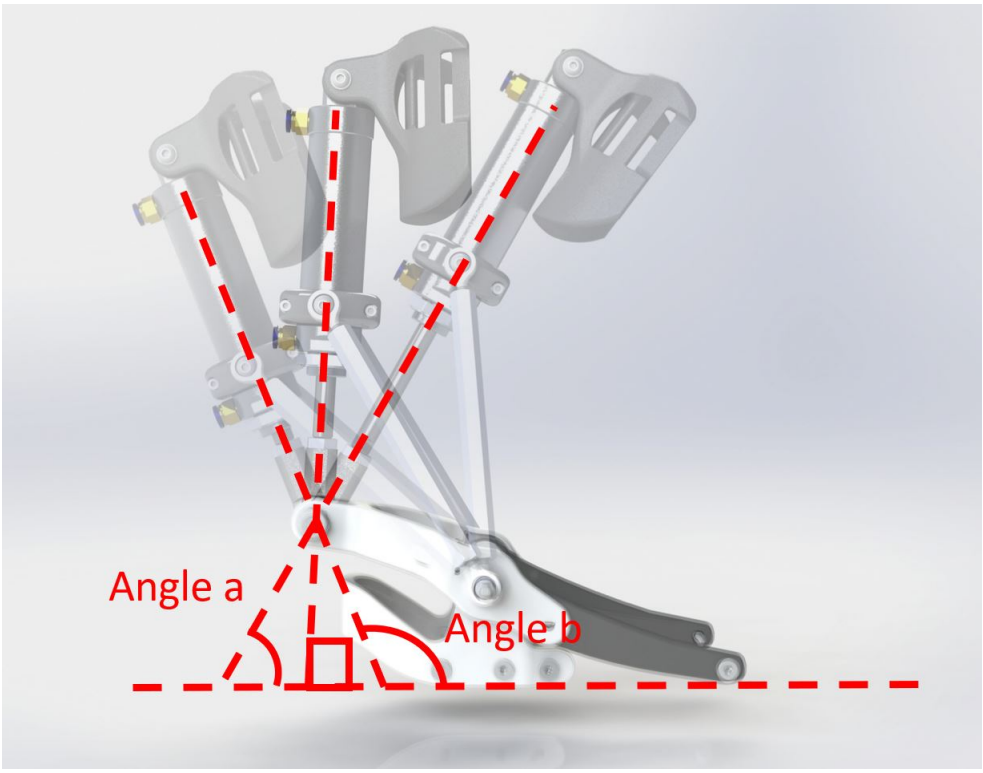

Figure 1.1: Maximum Variation of Angle for Plantar and Dorsi flexion

offering increased user comfort, affordability, and accessibility. The AAFO uses a lever arm that is free to pivot in the middle around a steel pin and is fixed at one end to the fore-end of the user's shoe on either side of the foot. The pivot point of the arm is secured to the hind end of the user's shoe, and the other end of the lever arm is attached to a double-acting air cylinder where retraction and extension forces are applied. Simple geometric relationships can be used to derive the relationship between input air pressure and maximum theoretical propulsive force.

$$F_{GR} = cos(\theta) \times P_{air} \times A_{cylinder} \times \frac{d_1}{d_2} \tag{1}$$

where, d_1 and d_2 is 99.06mm and 133.604mm, then

$$F_{GR} = cos(\theta) \times P_{air} \times 5.34 \tag{2}$$

The $A_{cylinder}$ is given square mm and F_{GR} is N. The application of the force on the mechanical parts of the design can be seen from figure 1.2. The equation above can

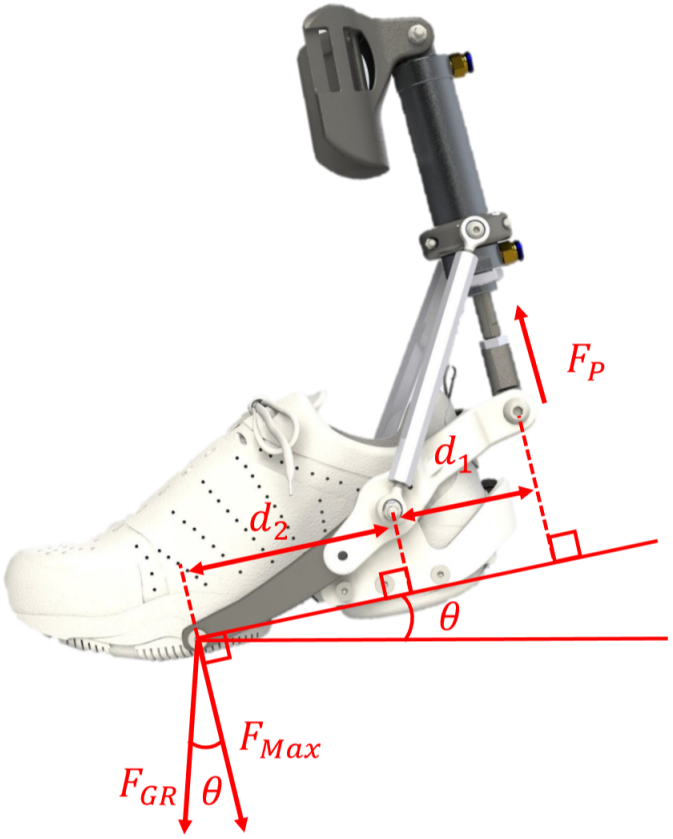

Figure 1.2: Geometric Representation of the Force Acting on the Shoe

be used to calculate the maximum theoretical propulsive force the AAFO. With a cylinder bore of approximately 32 mm and a maximum pressure of approximately 70 psi, the maximum theoretical force the AAFO is capable of providing is when theta is zero. Under these conditions, the maximum theoretical force is approximately 1661 N. To minimize the weight being added to the lower extremities, much of the pneumatic of the system were moved remotely to reduce the negative metabolic effects of increased weight to the lower legs. A Condor MOPC Modular Operator Plate Carrier (Condor Outdoor Products, Irwindale, CA) was used to house the pneumatic control

equipment for the suit including the air solenoids, batteries, and all electronics with the exception of the sensors and the AAFOs themselves. The Air solenoids used were Numatics 236-127B 24V 6Watt Solenoid 2-position a4-way valves (Numatics, Incorporated, Novi, MI), and were responsible for the control of the airflow through the system. The sensor casings and much of the AAFO parts with exception of the air cylinder and hardware were 3D printed in Polylactic acid (PLA) material. The double-acting air cylinder used was a Sydien Single Rod Double Action Pneumatic Cylinder (Chled, Zhejiang, China) with a 32mm Bore and a stroke of 75mm. Air was supplied via a commercial air compressor located remotely. A mobile air supply system would be similarly effective at delivering propulsive force as well and was successfully tested in non-recorded troubleshooting sessions. The mobile air supply system can be seen in figure 1.3. The design and orientation of the lever arm, linkage arms, and shank support provide a rigid connection between the shank and foot with minimal chafing or rubbing. The force of the air cylinder contracting is transferred through the level arm to the front of the foot, where the foot typically reaches maximum Plantar flexion at beginning of the swing phase, ensuring maximum propulsive force duration.

1.2.2 Design of the Electronic System

The AAFO uses an Adafruit Feather HUZZAH (Adafruit Industries, New York, NY) onboard to process and transmit the incoming IMU data for data analysis onto to computer via WiFi, as well as output control signals to two VNH5019 Motor Driver Carriers. The Motor Drivers are responsible for activating the air solenoid valves and control the pneumatic actuation of the AAFO. The IMUs used are two Adafruit (Adafruit Industries, New York, NY) BNO055 Absolute Orientation Sensors which are placed on the shank of the subjects using straps and custom-designed sensor housing.

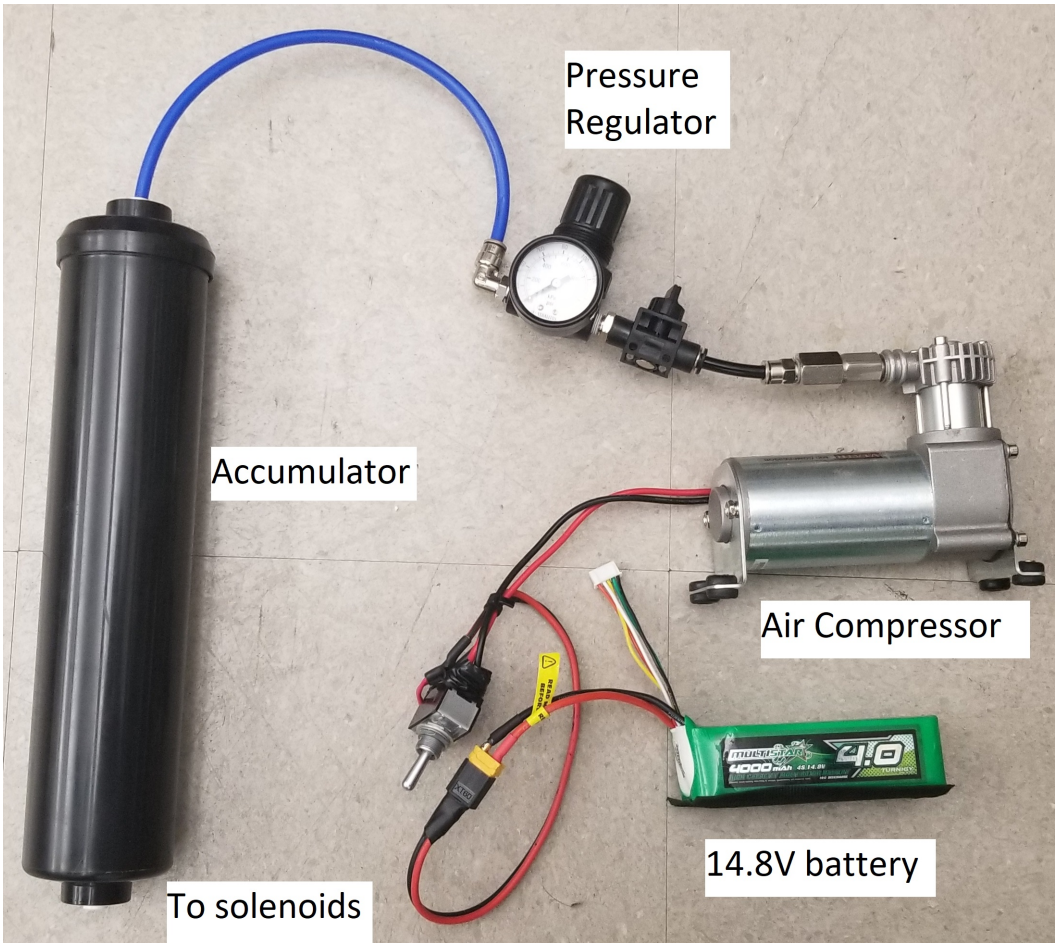

Figure 1.3: Mobile Air Supply System

The paper from Quintero et al Quintero *et al.* (2017) showed a similar application of using IMU sensors for detecting gait cycles for lower limb orthotics. The feather Huzzah is programmed using the Arduino IDE and a MATLAB (Mathworks, Natick, MA) script is developed to remotely acquire the data via WiFi. The IMU sensor is a 9-DOF sensor with a 3-axis accelerometer, gyroscope, and magnetometer.

Inertial Measurement Units: The BNO055 Absolute Orientation sensors are an sensors that has a built-in processing unit (i.e. high speed ARM Cortex-M0 processor) which is capable of measuring the absolute orientation, quaternions and euler angles from the 3-axis accelerometer, gyroscope and magentometers. It has been shown in

the paper by Wåhlin and Wrange (2018) that these sensors are effective in measuring the mobility of knee joints. The product specification of these sensors are given in the website by Adafruit (2020). This breakout board is capable of measuring Absolute orientation in Euler Angles, Absolute orientation in Quaternion, Angular Velocity vector, Angular and linear acceleration vector, magnetic field strength, gravity vector and ambient temperature. This sensor was selected over the others because of its versatile functionality and its in-built capability to output Absolute orientation in Euler angles and Angular velocity which are necessary for measuring the parameters that will be utilized in the device. In the figure 1.4, we see the BNO055 module in the custom 3-D printed housing. The housing is attached to the shank of the user using velcro braces. The sensor is oriented such that the flexion in the sagittal plane is in the y-direction.

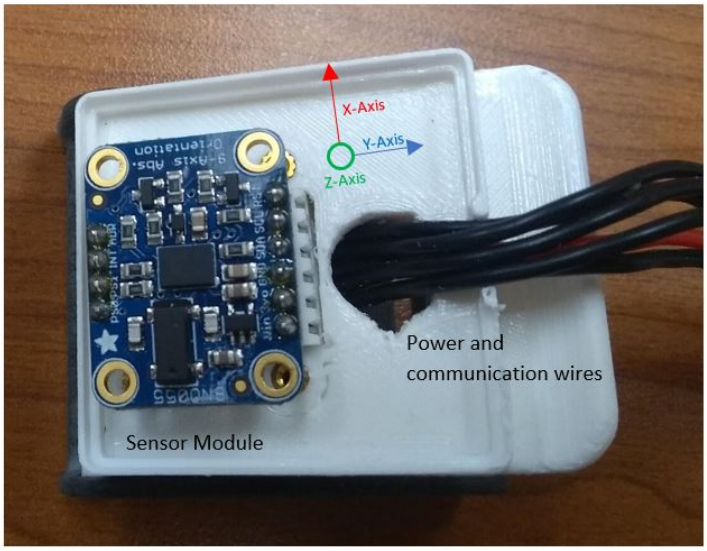

Figure 1.4: IMU Sensor in 3-D Printed Housing

1.2.3 System Block Diagram

In figure 1.5 we show the block diagram of the system. The V_1, V_2, V_3 and V_4 are the solenoid valves that control the actuation of two cylinders. The IMU's communicate with the Microcontroller on the I2C (Inter-Integrated Circuit) communication bus with clock and data lines. There is an internal 10k pull-up resistor on the IMU board. The pull-up resistors provide the default states of the signal lines.

Some of the negative factors of previous AAFO designs involved placing the bulk of

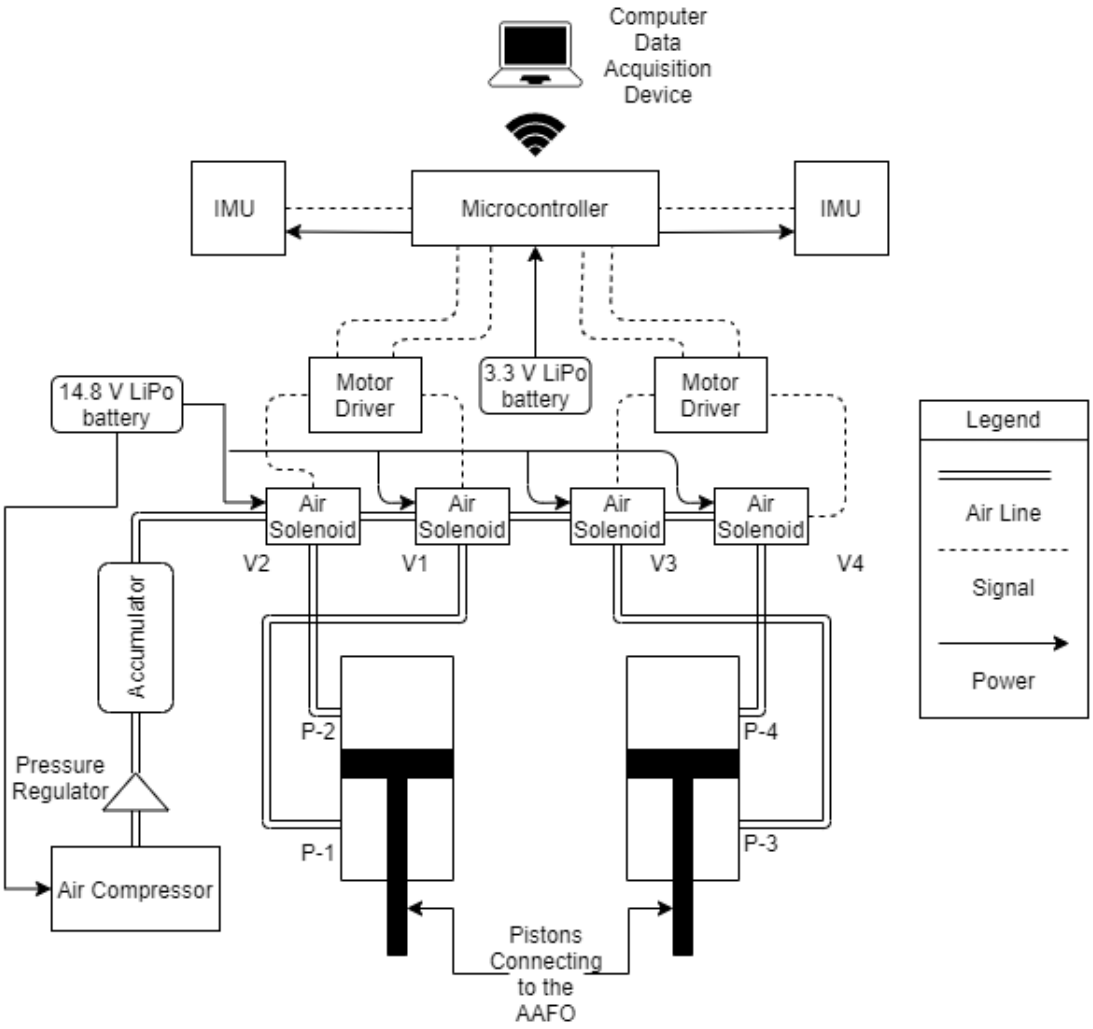

Figure 1.5: Block Diagram of the System

the heavier components on the ankle of the user. This led to an unnatural burden on the lower body to lift the extra weight during walking and would lead unnatural gait and increased metabolic cost. In this design, we aimed to displace bulk of the heavier components to the torso of the user away from the ankle such that ankle brace contains only essential components required for actuation. The figure 1.6 shows the device from the Front, Back and Side Views. The user is made to wear the condor modular plate carrier which houses all the electronics and the pneumatics portion of the device. The ankle braces are fitted to the user's shoe as described in the previous section. The IMU sensors are attached to the shank of the user using the custom made 3-D printed braces. Electrically insulated sheaths were used to house the wires running from the housings on the torso to the actuators and the sensors. The sheaths were attached loosely so that it doesn't inhibit the normal movement of the user. The entire design of the device is done by keeping in mind user comfort, unobtrusive usage and the ease of utilizing the daily footwear of the user.

1.2.4 Control Algorithm

We designed an algorithm 1 for controlling the actuation of the cylinder based on the Euler angle inputs from the IMU sensors. The V_1, V_2, V_3 and V_4 are the solenoid valves shown in figure 1.5. We used the connection diagram mention in Qi *et al.* (2019) for finalizing the solenoid connections. The control parameters defined in the algorithm are described as follows:

- α is the threshold angle for the absolute difference of the angles between the two IMUs. α_1 is the left shank angle and α_2 is the right shank angle with respect to the vertical plane from the sagittal side.

- λ is the flag that determines which leg needs to be actuated. It's set to 1

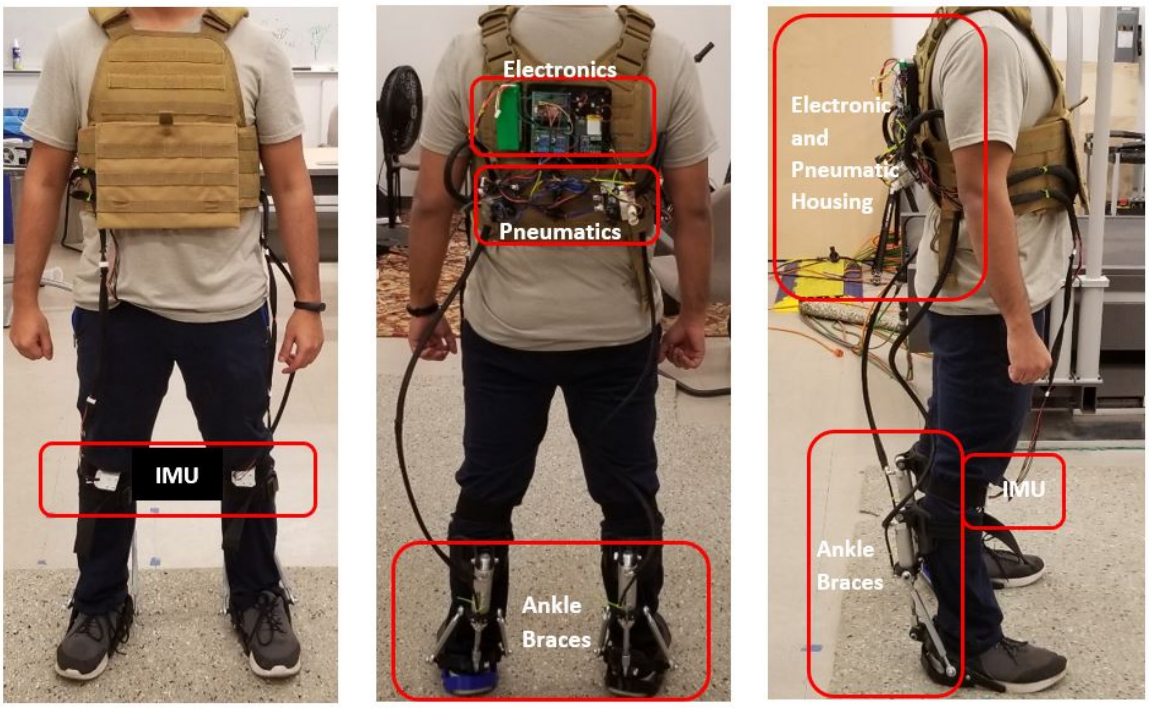

Figure 1.6: Front, Back and Side Views of the Device

left leg and 2 for the right leg. This ensures that a single leg is not actuated consecutively during a single gait cycle.

- τ is the time delay for the sensor read. This was set to the minimum amount possible for consistent data communication over Wifi for the Data Acquisition System.

- t_0, t_1 and t_2, these are time set for determining the various phases of the gait cycle. Since we conducted our experiment at a constant speed, the values remained constant throughout the experiment

In figures 1.7 and 1.8 we show the various phases of a single gait cycle as captured from the testing of the device by the subjects. The various phases shown are the 1) Double support, stance phase, 2) Loading Response, stance phase, 3) Mid Stance, stance phase, 4) Terminal stance, stance phase, 5) Pre-Swing (Push-off) stance phase,

6) Initial-Swing, swing phase, 7) Mid-Swing, Swing phase and 8) Terminal Swing (Heel-Strike) swing phase. The nomenclature of each of the phases was obtained from Taborri *et al.* (2016). Here the phases are labeled according to the left leg of the subject (i.e. the leg closer to the camera). The angle α is the angle difference between the two IMU sensors placed in front of the shank of the subject. The sensors provide the shank angle on the sagittal plane of the subject. Here α is the control parameter used in our control algorithm 1.

Algorithm 1 Control Algorithm for the Device

Initialize: Sensor system, Wifi module, calibration parameters, control parameters like α, λ,τ,t_0, t_1 and t_2.

Obtain offset values from calibration parameters for the sensors

while Client connected **do**

Obtain α_1 and α_2 from IMU sensors {Retrieve the euler angles from IMU sensors}

if $abs(\alpha_1 - \alpha_2) > \alpha$ **then**

if $\alpha_1 < \alpha_2$ and $\lambda \sim= 1$ **then**

Activate V_1 {Extend Left leg for push off}

Start counter $t = t_1$

Set $\lambda = 1$ {Here $lambda = 1$ indicates left leg}

else if $\alpha_1 > \alpha_2$ and $\lambda \sim= 2$ **then**

Activate V_3 {Extend Right leg for push off}

Start counter $t = t_1$

Set $\lambda = 2$ {Here $lambda = 2$ indicates right leg}

end if

else

Deactivate V_1, V_2, V_3 and V_4 {Free move state}

end if

Reduce counter t

if $t < t_2$ **then**

if $\lambda = 1$ **then**

Activate V_2 {Retract Left leg for heel strike}

end if

if $\lambda = 2$ **then**

Activate V_4 {Retract Right leg for heel strike}

end if

end if

wait for τ ms {Delay for sensor read}

end while

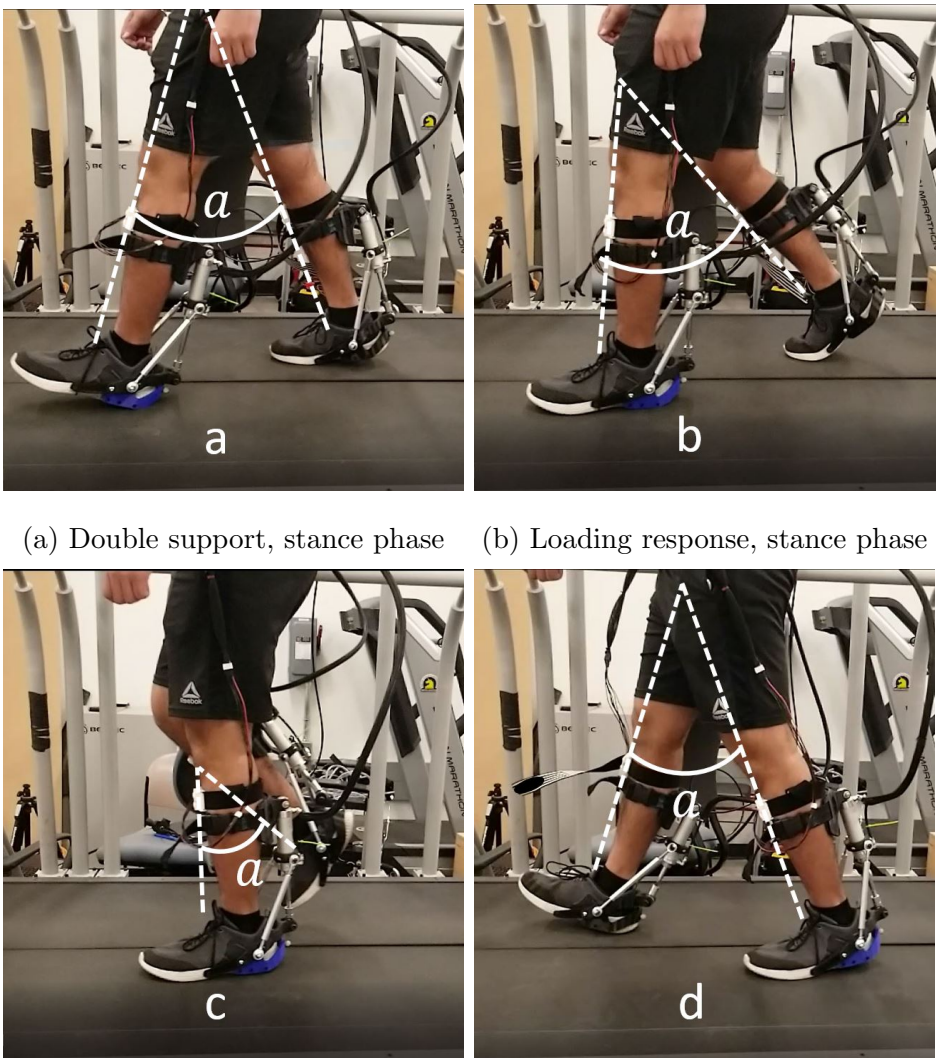

(a) Double support, stance phase

(b) Loading response, stance phase

(c) Mid stance, stance phase

(d) Terminal stance, stance phase

Figure 1.7: A Single Gait Cycle With 8 Level of Granularity – First 4 Phases

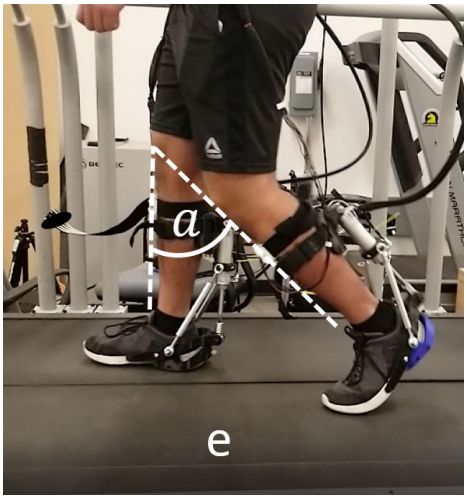

(a) Pre swing (Push-off), stance phase

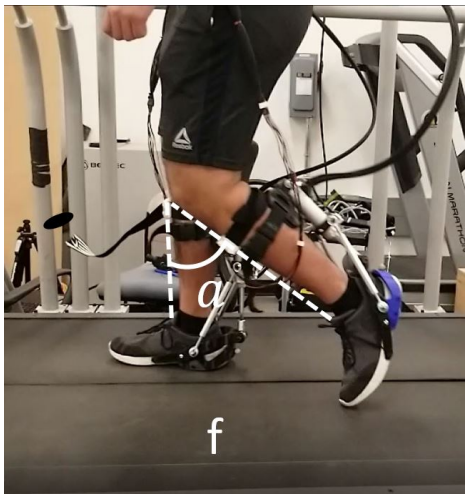

(b) Initial Swing, swing phase

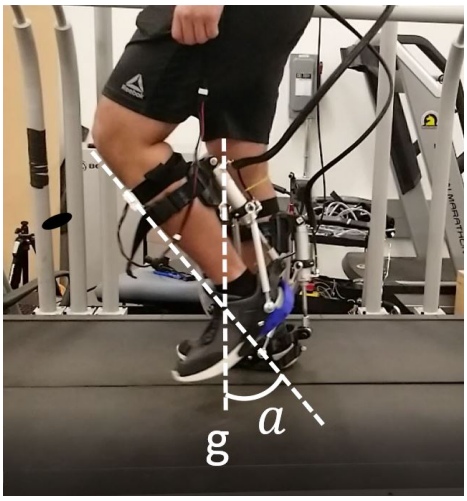

(c) Mid Swing, Swing phase

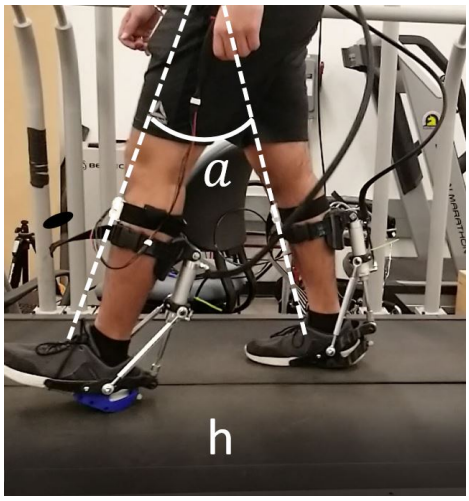

(d) Terminal Swing(Heel strike), swing phase

Figure 1.8: A Single Gait Cycle With 8 Level of Granularity – Last 4 Phases

We obtain the shank angle measurements as shown in figure 1.9. Similar to the approach in Watanabe *et al.* (2011), the angle variation of the shank for each phases of the gait cycle is calculated and using those values we were able estimate the timings for actuation of the cylinders. We also confirmed the estimated values with the data obtained from our IMU sensors as shown in figure 1.9 by observation during the habituation phase of the subjects to determine the values for the control parameters α, t_0, t_1 and t_2. These values were also adjusted according to the comfort of the subjects.

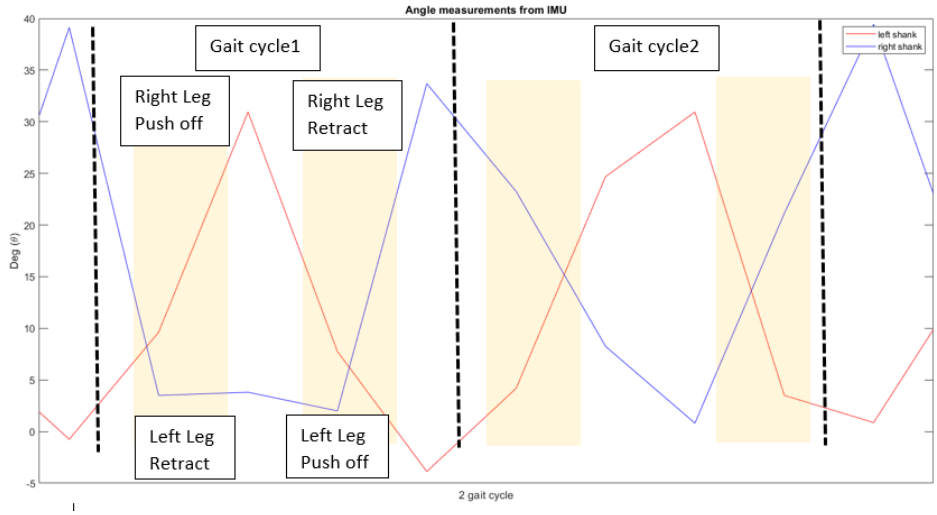

Figure 1.9: Shank Angle Measurements From IMU Sensors

1.3 Results and Discussion

1.3.1 Procedure for Testing the Device

We conducted a preliminary test of our device's ability to provide a stronger plantar flexion, we used 4 subjects on an instrumental dual-belt treadmill with force sensors (Bertec, Columbus, Ohio). The subject was fitted with the device on both of their legs and was made to wear the condor plate carrier with all the additional

equipment. The testing phase had two sessions.

- **Habituation Test for acclimatization to the device**: In their first session the subjects were fitted with the AAFO and was made to walk on the ground for 5 minutes to habituate themselves with the device. They were given 10 minutes on the treadmill with varying speeds between 0.5 m/s to 1.2 m/s to acclimate themselves to the shoes for the final testing session. During their habituation time on the treadmill, data of their shank angle variation was collected from the IMU sensors for estimating their plantar flexion time and their swing phase time for synchronizing the actuation of the cylinders. The source pressure was varied from 30 psi to 70 psi and the subjects were notified about the pressure level allowing them to anticipate the assistance from the device.

- **Walking test for collecting ground reaction force**: In their second session, the subjects were instructed to walk on the treadmill for 1 min with a normal walking speed of 1 m/s. A passive reflective heel marker was placed on both the heels of the subject to determine the heel-strike event on the treadmill. The motion of the heel marker was captured using a motion capture system (Vicon, Oxford, UK) at 1000 Hz. There was 4 pressure condition used for testing the ground reaction force: 1) No pressure, 2) Pressure at 30 psi, 3) Pressure at 50 psi, 4) Pressure at 70 psi. Ground Reaction Force (GRF) was collected for each of the pressure used.

We used young healthy subjects of similar age group without any impairments for the purpose of this preliminary test. Subject information can found in Table 1.1.

Table 1.1: Subject Attributes

Attributes	Sub_A	Sub_B	Sub_C	Sub_D
Height(cm)	177.8	172.2	177.8	185.4
Weight(kg)	88.45	87.54	87.99	112.35
Age	20	25	25	25
Shoe size(US)	11.5	9.0	9.5	12.0

1.3.2 Results of Testing

The figures 1.10, 1.11, 1.12 and 1.13 represents the Anterior-Posterior GRF obtained from the left leg of the 4 subjects. The initial data from the motion capture system was processed in the Vicon Nexus software (Vicon, Oxford, UK), where the markers were labeled and gaps were filled with a custom plugin. The data was then extracted and further processed on the Matlab software (MathWorks, Natick, MA). The raw data was initially filtered with 2nd order low pass Butterworth filter of 10 Hz. The heel strike events were calculated by finding the recurrence of the least angle of the heel marker. The individual gait cycles were then extracted from the filtered data, curve fitted and an average of 5 gait cycles was taken to obtain the average plots. The plots show the GRF obtained for the 4 pressure conditions. The red line indicates the GRF at 0psi, the green line indicates GRF at 30psi, the blue line indicates GRF at 50psi and the black line indicates GRF at 70psi. The GRF data of Subject D at 70psi was a bad trial and was excluded from the plots. The initial trough in the plots is the Braking force applied by the stepping leg to go from the swing phase of the gait cycle to the stance phase after heel strike. The peak that follows from the trough represents the Propulsive force that the stepping foot generates to transfer from the

stance phase to the swing phase of the gait cycle.

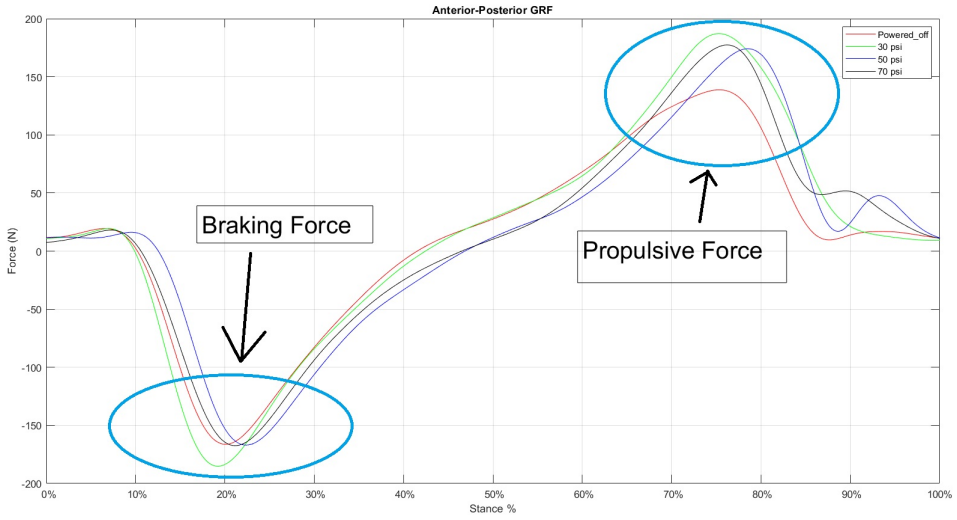

Figure 1.10: Anterior-Posterior GRF of Left Leg of Subject A

1.3.3 Discussion of the GRF Data

The results from this preliminary testing of the device show that there is a trend of higher GRF during propulsion with an increase in supply pressure added to the cylinder. For the purpose of this experiment we only analyze the left leg GRF, however during the experiment the subjects were wearing the device on both legs to induce symmetry. This trend of increasing GRF with an increase in force is attributed to the force applied to the ball of the foot by the device during push-off. The additional push-off force increased the anterior-posterior propulsion of the stepping leg. The results from subject A in figure 1.10 show that the highest increment of GRF from powered off condition was when a pressure of 30 psi was applied. The particular subject revealed during post-session that it felt the most comfortable with 30psi pressure. Subject B, C, and D all expressed that they could feel a higher push-off force with the increase in pressure. We show the GRF for individual subjects as

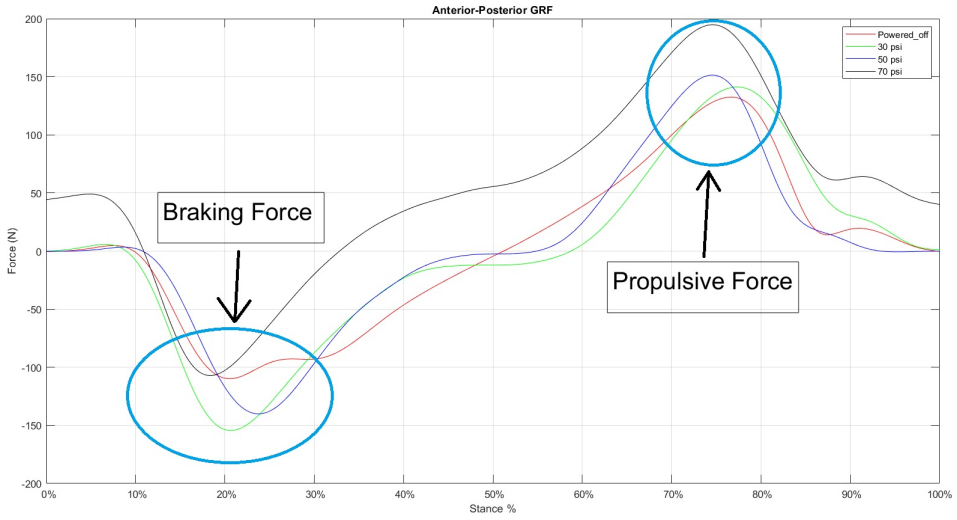

Figure 1.11: Anterior-Posterior GRF of Left Leg of Subject B

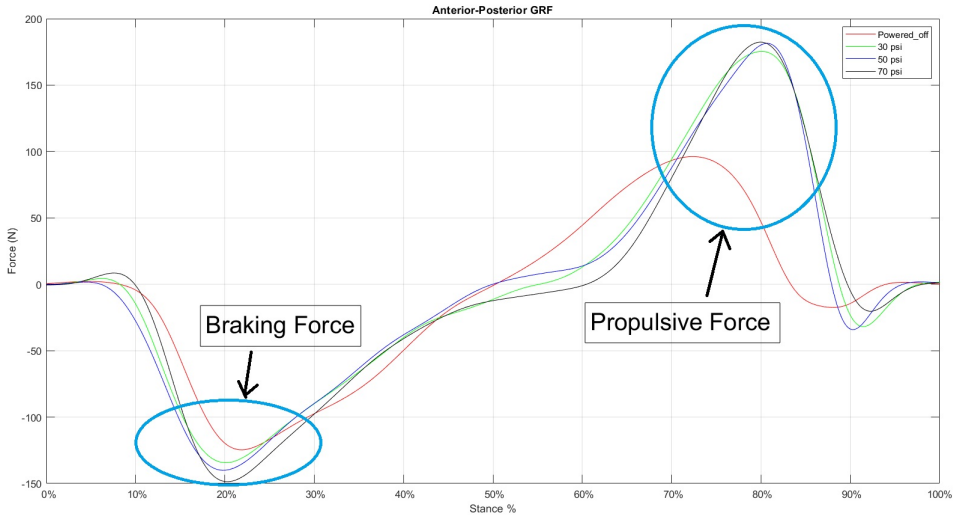

Figure 1.12: Anterior-Posterior GRF of Left Leg of Subject C

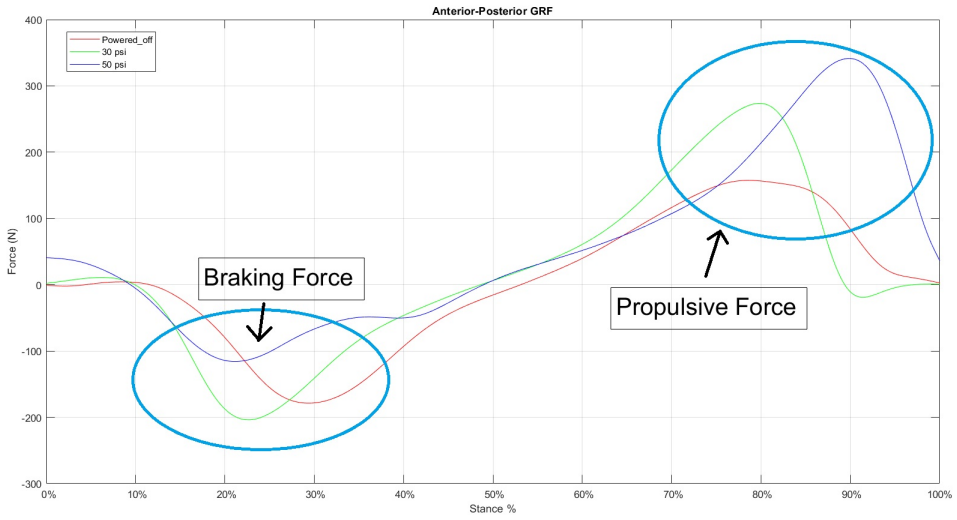

Figure 1.13: Anterior-Posterior GRF of Left Leg of Subject D

there was a high percent variation of the propulsive forces at their peaks. Subject A had a variation between 34.87% to 25.43% increase in GRF for the three different applied pressures. Subject B showed a variation between 6.5% to 47% increase in GRF for the different pressures. Subject C showed a variation between 82.44% to 89.61% increase in GRF with the different pressures. Subject D showed a variation of 42.4% to 116.8% increase in GRF with different applied pressures. Different control parameters as mentioned in algorithm 1 were used for different subjects and that could have attributed to the high variation of peaks of the propulsion force. Further testing of the AAFO on additional subjects might show an apparent trend in the relationship between the increase of pressure, control parameters, and the GRF.

1.4 Conclusions

In this chapter, we designed an Active Ankle-Foot Orthosis capable of increasing ground reaction forces of the user by applying a strong push-off force. The design is cost-effective and comfortable for the user. Individuals who have suffered from stroke

have a higher risk of falling and this device can potentially help them rehabilitate to improved living. There is evidence that with an active ankle-foot orthosis that can provide a strong plantarflexion force to the ankle, the individuals would be able to mitigate the factors that cause them to fall. The design of our device utilizes easy to use components and a novel control algorithm to provide a stronger push off during normal gait, such that the individuals wearing the device would be able to generate a stronger ground reaction force. Evidence from other studies suggests that a stronger ground reaction force would help in better forward propulsion and would help individuals take faster compensatory steps, increase their stride length, and potentially reduce chances of falling. Preliminary tests on the 4 different subjects show a general trend of an increase in the anterior-posterior ground reaction forces. There is a need for comprehensive testing of the device to fine-tune the control parameters and validate the effectiveness of the device, such that it can assist in the rehabilitation of people with impairments. An analysis of the treadmill perturbation data is performed in chapter 2 to potentially determine more effective control parameters like the threshold of the angular displacement of the shank, the timing for actuation of the shank that can successfully determine whether the stepping response will be a fall or a recovery. Additionally, the analysis will also help in determining the necessary kinematic parameters that can detect whether a second stepping response is required. The control algorithm of the device can then be adjusted such that the device only actuates when a stepping response is determined to be a fall by the IMU sensors. The device can then potentially reduce the chances of falling in individuals who are at high risk.

Chapter 2

ANALYSIS OF PERTURBATION DATA ON FALL AND RECOVERY

2.1 Introduction

The majority of techniques used for detecting falls requires the use of some kind of sensors to detect the event of a fall in the stepping response of the user. These sensors can be broadly classified into two categories of wearable and non-wearable sensors. The studies conducted by Chaudhuri (2015) shows a comprehensive list of available sensors used for detection of fall in older adults. The wearable sensors are analyzed in details by Chander *et al.* (2020) which includes, angle measurement potentiometers, electronic goniometer, foot pressure sensors, pedometer, accelerometers and gyroscopes as shown in studies Mukhopadhyay (2015), Light *et al.* (2015), Chen *et al.* (2005) and Shany *et al.* (2012). The non-wearable sensors include motion capture sensors, cameras, acoustic sensors, floor pressure sensors as shown in studies Sixsmith and Johnson (2004), Li *et al.* (2012), and Alwan *et al.* (2006). The negative factor for the use of non-wearable sensors is that it requires the user to be in a controlled environment where the sensors are placed. Restricting the movement of the user is not ideal since it hampers the quality of life experienced by the user. The majority of the active devices use wearable sensors for the detection of falls as shown by Chander *et al.* (2020). However, wearable sensors like angle measurement sensors or foot pressure sensors are restricted in their ability to detect a variety of changes in lower limb kinematics and therefore is not robust enough to detect falls in a variety of scenarios, such that it can be effective during daily user activity. Wearable sensors such as IMUs, accelerometers, and gyroscopes are effective in detecting kinematic

changes of the various body parts and can be continually used for detecting sudden changes of angular displacement or velocity during the user's daily activities. In order to utilize the IMU sensors effectively in fall detection, a detailed analysis of kinematic parameters that can be measured by these sensors needs to be performed.
The **objective** is to analyze the kinematic parameters of users during treadmill-based perturbations to determine effective sensor placement and potential parametric thresholds that would distinguish the stepping response between falls and recoveries. Additionally, it can also be used to determine whether the first stepping response was sufficient or actuation of the second leg is necessary. It is **hypothesized** that out of the multiple lower body kinematic parameters that can be measured, there exists a subset of those features that can be used to determine whether a sudden perturbation during stance phase would result in a fall or recovery.

In this chapter, the kinematic data collected by Nevisipour (2019) from clinical experiments that involve giving treadmill perturbations to subjects are analyzed. The objective is to find out the kinematic parameters that can most significantly differentiate between fall and recovery. The data is collected from individuals with unilateral chronic-stroke. The data from individuals from stroke is taken as they are the population at the highest risk of falls as mentioned by Jørgensen *et al.* (2002). In the subsequent sections, the methodology of data collection is described and an overall description of the data collected is also covered. The data analysis involves using statistical techniques like correlation, classification, and times series analysis on the kinematic variables like angular displacement and angular velocity. The major body parts used for measuring the kinematics are the trunk, knee, shank, foot, and hip. As stated in the hypothesis, that there should exist a subset of these body parts from where we can measure the angular displacement or velocity to determine

whether a perturbation will cause a fall or recovery. The subset of features thus, found can be used for placing the IMU sensors such that the device can successfully detect if the user is about to fall and can actuate to potentially prevent the fall based on the methodology described in chapter 1.

2.2 Methodology

2.2.1 Data Collection

The data was collected by Nevisipour (2019) in the Human Mobility Lab at ASU. In the study, there were forty-two individuals with unilateral chronic stroke and they are screened based on a eligibility criteria. The eligibility criteria was 1) ability to walk 5 minutes without assistance, 2) no spinal/lower limb injury/surgery in the past year, 3) no history of fainting in the past year, 4) at least a month of usage of a assistive device like a orthosis or functional electrical stimulators on a daily basis. This study was performed under the IRB approved protocol STUDY00002970 and all subjects provided written informed consents.
Subject data like age, height, weight, and stroke type were recorded. Various clinical tests were performed to evaluate the clinical characteristics of the subjects.

- **Fugl-Meyr Test**: The lower extremity impairmment was assessed.
- **Modified Ashworth Scale**: Spasticity of the ankle plantarflexors (lateral Gastrocnemius and Soleus) and dorsiflexor (Tibialis Anterior) was assessed.
- **Maximum voluntary isometric contraction (MVIC)** The plantarflexion and dorsiflexion was measured using a Biodex System 3 (Biodex, New York, USA).
- **Berg Balance Scale (BBS)** Functional Balance clinical test was assessed.

- **Timed Up and Go (TUG)** Functional Mobility Test was assessed.
- **10m Walk Test** Functional Mobility test was assessed.

The above set of tests were performed to match the groups and though an independent samples t-test for age, height and weight. They were further matched by stroke type and gender using a chi-squared test. Fugl-Meyer score, normalized MVIC for plantar- and dorsi flexion, Modified Modified Ashworth Scale, clinical scores of balance and mobility (BBS, TUG, 10 m walk test) were compared between the groups using an independent samples t-test.

The subjects were fitted in a safety harness and then treadmill perturbations were provided which required them to take single or multiple steps to prevent falling. The perturbations were provided in a way that would evoke forward or backward stepping respectively. For the purpose of the thesis only the trials with posteriorly- directed perturbations were considered. However, anteriorly- directed perturbations were provided randomly in the experiments to eliminate anticipations. The experiments were performed on a dual-belt treadmill (GRAIL, Motek Medical BV, Amsterdam, Netherlands). The subjects were asked to take a walk for 2 minutes with self-selected comfortable walking speed for the purpose of acclimatization to each conditions. The subjects were then asked to stand upright on the treadmill with a comfortable stance width. The subjects would stand with the same stance width before every trial.

There were three levels of posterior perturbations, i.e., level 1: small, level 2: medium, level 3: large. The stepping threshold were decided based on the previous studies (Owings *et al.* (2001)). All the perturbations were provided with a trapezoidal velocity profile according to the previous studies conducted in older adults (Honey-

cutt *et al.* (2016)) and individuals with stroke (Crenshaw and Grabiner (2014)). The velocity profiles are explained in table 2.1, 'BW' stands for Body Weight. A sample

Table 2.1: Velocity Profiles of the Dual Belt Treadmill

Levels	Displacement (m)	Constant Velocity (m/s)	Acceleration (m/s^2)	Deceleration (m/s^2)
level 1	17% of BW	1.00	10.0	-10.0
level 2	32 % of BW	1.26	12.6	-12.6
level 3	47.5% of BW	1.26	12.6	-12.6

velocity profile of subject with height 170 cm is show in figure 2.1. The experiments

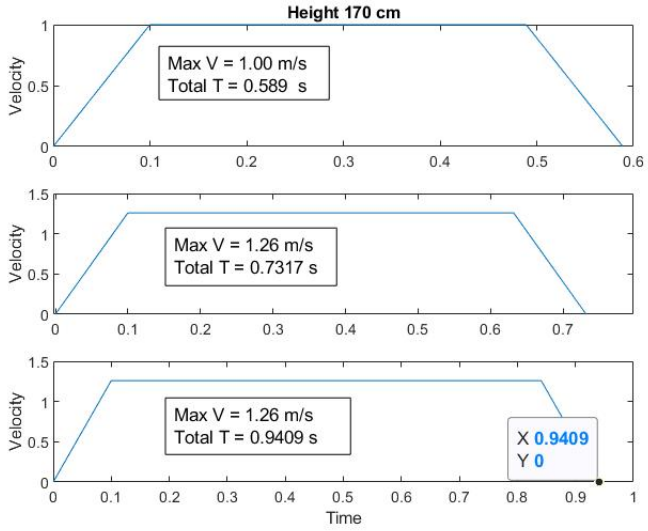

Figure 2.1: Velocity Profile of Subject With Height 170 Cm

were performed in three rounds. In the first round, 3 posterior and 2 anterior perturbations were provided, randomized in direction but in the increasing order of intensity for safety reasons. Two more rounds of the same intensity was provided in a com-

pletely randomized fashion. The performance of the subjects were observed at each trials for each round. If the subject fell (i.e. unambiguously caught in the harness) on any perturbation level, the same perturbation level was repeated up to 3 times. If the subjects fell on all 3 trials, no more perturbation of that level or larger was delivered (i.e. that level or larger ones were removed from round 2 and 3).

The subjects were fitted with passive reflective markers according to the modified Helen Hayes Marker Set (Kadaba *et al.* (1990)) and the trajectory for each of the markers were recorded using a 10-camera motion capture system (Vicon, Oxford, UK) at 250 Hz sampling rate. The data was post-processed using the Vicon Nexus 2.6.1 (Vicon, Oxford, UK), a 4th order Butterworth filter with a 6 Hz cutoff frequency was used to the kinematic data of the markers. Ground Reaction Forces were also calculated through the force plates (Bertec, Columbus, OH) embedded in the treadmill under each belt.

2.2.2 Data Description

The marker data, which are time series data for each trial was first filtered and then processed using MATLAB software (Mathworks, Natick, MA). The marker data contained events like **Treadmill start, Step start and Step stop** which were identified manually using the Vicon Nexus software. The overall kinematic data can be categorized into 3 major components.

1. **Overall Kinematic Parameters**: Reaction time, Step time, Step length, Step length, Step width, Change of Step width, Pre-Step width.

2. **Kinematics of Individual Body Parts**: Center of Mass to Base of Support distance, Angular displacement and angular velocity of Margin of Stability

(MOS), Trunk, Shank, Ankle, Knee, Hip, Foot for both the stepping and base legs.

3. **Kinetic Parameters**: Stepping WB, Base WB, peak push off vertical direction, peak push off shear, peak foot strike vertical, peak foot strike shear, push off impulse, Total Moment, Support Moment, Initial Moment.

The description of the above dependent variables are given in table 2.2. The Angular displacement and angular velocity time series data of each individual trials were also collected for further processing and analysis. The primary body parts from which the angular displacement and angular velocity were extracted was **Ankle, Shank, Trunk, Knee, Hip and Foot**. For each of these body parts the angular displacement and angular velocity was recorded at step start and step stop. There were a total of 7 features for the overall kinematic parameters, 57 features for the individual body parts kinematics and 10 features for the kinetic parameters. During the data collection it was recorded whether the individual had a fall and recovery. This would be referred in the document as the fall parameter where its given the value 1 if the person had fallen during the particular trial and the value 0 if the person had recovered during the particular trial. This information was used to classify the data into categories of fall and recovery and to correlate them against the above mentioned parameters. The time series data for the individual trials were then processed and the parameters in table 2.3 were extracted. These variables were obtained by first calculating the mean of the individual trials and then a overall mean for each individual body parts.

Table 2.2: Dependent Variable Description

Variables	Description
Reaction Time	The time from the onset of perturbation to Step start.
Step Time	The time from Step start to Step stop of the stepping leg
Step Length	The anterior-posterior displacement between stepping and base leg foot centres at Step stop
Step Width	The width of the two legs at the start of perturbation.
Change of Step Width	The difference in width of the two legs at the start of perturbation and end of perturbation
CMBOS (x and z)	The anterior-posterior and vertical displacement between center of mass and base of support at step stop
Margin of Stability (MOS)	Dynamic stability measure calculated using both position and velocity of CM relative to the edge of BOS.
Stepping WB	Weight Bearing Asymmetry : % of weight put on stepping leg 500ms before perturbation.
Base WB	Weight Bearing Asymmetry : % of weight put on base leg 500ms before perturbation.
Peak Push-off	Maximum Ground Reaction Force (GRF) during propulsion in both the vertical and anterior-posterior direction.
Peak Foot-Strike	Maximum Ground Reaction Force (GRF) during braking in both the vertical and anterior-posterior direction.
Moment	The moment on the body at Step stop with respect to the Base of Support

Table 2.3: Variables From Time Series Data

Variables	Description
Max Angle	Maximum Angular deflection during a trial.
Max Angle Time	The % of gait at which max angle deflection occurs.
Max Velocity	Maximum Angular Velocity during a trial.
Max Velocity Time	The % of gait at which max velocity occurs.
Min Velocity	Minimum Angular Velocity during a trial.
Min Velocity Time	The % of gait at which min velocity occurs.
Rise velocity time	The % of gait it takes for velocity to reach its max
Fall velocity time	The % of gait it takes for velocity to reach its min

2.2.3 Data Processing

The aim of processing the above data-set is to determine the **kinematic features** that are primarily responsible for causing a person to fall or recover from the given perturbations in a trial. The attempt is to reduce the number of features such that it is convenient to obtain the data using external sensors like Inertial Measurement Units (IMUs). This information can then be used to support the design of the device mentioned in chapter 1 for detecting beforehand whether the user is going to fall or recover from a perturbation. The data processing of the overall data was divided into multiple parts.

Correlation Analysis: Initially, it's determined as to which of the parameters from the 3 different categories mentioned above, is highly related to the fall parameter

(i.e. the person has fallen or recovered in the particular trial). In order to achieve this analysis, a correlation analysis is performed. A Pearson product moment correlation co-efficient Mukaka (2012) is calculated for the three categories of the features with respect to the fall parameters. The co-efficient is calculated as described in equation 2.1

$$r = \frac{\sum_{i=1}^{n}(x_i - \bar{x})(y_i - \bar{y})}{\sqrt{\sum_{i=1}^{n}(x_i - \bar{x})^2}\sqrt{\sum_{i=1}^{n}(y_i - \bar{y})^2}} \tag{2.1}$$

The results from the correlation analysis is given in tables 2.4, 2.5,and 2.6. It's to be noted that the correlation coefficient is between -1 and 1, with closer to 1 would suggest high positive correlation, close to -1 would suggest high negative correlation and closer to 0 would suggest low positive/negative correlation. Out of the 3 different categories, the features from the Kinematics of Individual Body Parts are the most helpful for placing the potential sensors since each of the features corresponds to a physical body part. Hence, the highly correlated features from this category are most prominently visited in this thesis.

Classification Analysis: In order to determine whether the above features from all the 3 different categories are sufficient to classify the individual trials into falls and recoveries, a logistic regression model from McCullagh (1989) is developed using the features from the above 3 categories and the fall parameter as label. Since we have a binary classification between whether a subject has fallen (fall parameter = 1) or has recovered (fall parameter = 0), logistic regression is an effective model for prediction of such classes. The open-sourced sci-kit learn package of Python using Jupyter notebook is used to perform the classification. The overall data is split into 75% training set and 25% validation set. In order to evaluate the performance of the classification model, the scores such as precision, recall and f-1 (Goutte and Gaussier (2005)) are used. The evaluation scores (Shung (2018)) are described as:

- **Precision**: This is a way of determining how good precise the model is in predicting the actual positive values. It is a good percentage measure when the cost of false positive is high.

$$precision = \frac{TruePositive}{TruePositive + FalsePositive}$$

- **Recall**: It determines the percentage of actual postive values that the model is able to capture through labeling as true positive. This applies best to the model which has high cost associated with the false negatives.

$$recall = \frac{TruePositive}{TruePositive + FalseNegative}$$

- **F-1**: This is the harmonic mean of precision and recall. It's useful in seeking a balance between both the above metrics. Since in our case we do not have an even number of falls and recoveries, we will be relying on this metric for evaluation of our model.

$$f1 = 2 \times \frac{precision * recall}{precision + recall}$$

The data obtained from the above classification analysis is shown in table 2.7 and 2.9 Once the correlation and prediction accuracy is performed, the individual body parts with the highest correlation to the fall parameters are determined. These individual body parts are then further analyzed using the angular displacement and angular velocity time series data for individual trials.

Time Series Analysis: For the purpose of this thesis, the time series data of both angular displacement and angular velocity are obtained from the trials of 11 subjects. In the overall dataset that was processed for the thesis there were 28 fall trials and 29 recovery trials. The subjects which had approximately equal falls and

recoveries in their trails were selected for this analysis. The data was first categorized into falls and recoveries for individual subjects based on the fall parameter. The time series plots were sliced based on the treadmill start indices and step stop indices that were determined from event data file that was obtained for every trial. This was done in order to locate the time series for an individual gait cycle. The individual gait cycles for all the trials were then extracted and were fitted using smoothing spline function in MATLAB software. All the gait cycles were interpolated to 10000 samples to achieve a uniformity in the dimensions. The average of the time series were then calculated for the individual subjects and then for all the subjects together based on fall and recovery categories. A confidence interval of 95% was obtained around the mean to determine the accuracy of the overall data. The average of the overall time series data is representative of the angular displacement and angular velocity of a typical fall and recovery for each of the correlated individual body parts. The table 2.3 describes the various time series variables that were used in the final analysis.

2.3 Results and Discussion

Results From Correlation Analysis The results from the correlation between the 3 different categories with the fall parameter are observed in this section. Since the fall parameter is 1 for a fall trial and 0 for a recovery trial, the coefficients with a higher positive value would mean the higher the value of the feature would contribute to more falls in subjects. The coefficients with higher negative value would mean the higher the value of the feature would contribute to more recoveries in subjects. In the table 2.4 we see the correlation between the overall kinematic parameters with falls. The reaction time parameter shows a higher positive correlation of 0.33 to fall which suggests that subjects with faster (smaller) reaction time will most likely recover from the perturbation. The Step Time parameter is the time of the stepping

leg in the air during a step and it has a negative correlation of -0.42 to fall which suggests that subjects who took a longer time from step start to step stop are more likely to recover. The Step Length parameter also has a negative correlation of -0.37 with the fall parameter and that is consistent with the step time, since it's highly probable that subjects who were able to keep their stepping leg in the air were able to take a longer step. In the paper by Nevisipour and Honeycutt (2020) it's shown that a longer step length leads to a reduction in trunk velocity, which suggests that the subject was able to arrest their fall by increasing the base of support. This also suggests that while the stepping leg was in the air, the base leg was able to provide sufficient stability which is crucial since the base leg needs to support the weight of the whole body momentarily while the stepping leg is in the air.

Table 2.4: Correlation Between Overall Kinematic Parameters With Falls

	Reaction Time	Step Time	Step Length	Step width	Change of step width	Pre-Step width
Fall	0.33	-0.42	-0.37	0.13	0.045	0.13

In the table 2.5 and 2.6 we observe the positive and the negative correlation between the kinematics of the individual body parts with the fall parameter. In order to reduce the number of features for the time series observation, we take the body parts which has a high correlation with fall and whose angular data can be conveniently calculated using sensors attached to the body. In the positive correlation table 2.5 we see that the shank angle at step stop has the highest correlation (0.65) with fall. The subsequent correlations shows that the Foot angle (0.60), Trunk velocity (0.55), Hip velocity (0.52) and Knee angle (0.47) also have a high correlation with the fall

parameter. It suggests that a higher value of these parameters increases the chances of falls in the subjects. We observe the time series data of the above body parts to see if there is a way of predicting the fall before it occurs. In the negative correlation table 2.6, we observe that the the anterior posterior distance of the Center of Mass Base of Support(CMBOS) at Step Stop has the highest negative correlation (-0.60) with the fall parameter which is consistent with the fact the step length also had a higher negative correlation with the fall parameter. The Margin of Stability (MOS) is the dynamic stability of the body measure which is positive if its stable and negative if its unstable. It also higher negative correlation (-0.48) with the fall parameter since a stable margin would have a higher positive which leads to a recovery. In this thesis, we use the body parts corresponding to the positive correlation for our time-series analysis since it will be more convenient to attach sensors to them and obtain the required angular displacement or velocity data.

Table 2.5: Positive Correlation Between Kinematic Parameters of Individual Body Parts With Falls

	Shank Angle at Step Stop	Foot Angle at Step Stop	Trunk velocity at Step Stop	Hip velocity at Step Stop	Knee Angle at Step Stop
Fall	0.650555	0.602187	0.545221	0.522828	0.470711

Results from Classification Analysis The results from the classification model - logistics regression is observed in this section. In the table 2.7 we see the report of the classification using the overall kinematic parameters. Here we observe that the precision value (0.79 and 0.71) is lower which suggests that there are lot of false positive, (i.e. its classified as a fall when it was actually a recovery). The recall value

Table 2.6: Negative Correlation Between Kinematic Parameters of Individual Body Parts With Falls

	CMBOSx Step Stop	MOS Step Start	CMBOSx Step Start	MOS velocity Step Start	CMBOSz velocity Step Stop
Fall	-0.604765	-0.484238	-0.466704	-0.462899	-0.462325

is high for recovery class (0.96) which suggests that its able distinguish when its a Recovery, but has a low recovery value with the fall class which suggests that it fails to find the false negatives during fall. The table 2.9 reports the classification scores

Table 2.7: Classification Report Using Overall Kinematic Parameters

Classes	Precision	Recall	F-1
Recovery	0.79	0.96	0.87
Fall	0.71	0.29	0.42

using the Individual Body Parts Kinematics. We observe that both the Precision is high for both fall and recovery (0.96 and 0.88) which suggests that the model is successful in its prediction for majority of the time using only these features. It is able to clearly detect the false positives for both fall and recovery. The recall is high for both fall and recovery (0.96 and 0.88) as well which suggests that the model is successfully distinguishes between the false negatives. The overall high F-1 score for both falls and recoveries suggests that these parameters are useful in separating the data from falls and recoveries. In order to reduce the number of features for our time series analysis, we observe the coefficients of the final logistic regression

hypothesis function. We observe only those body parts which had a high correlation with the fall parameter in the correlation analysis in table 2.8. The mean of the coefficients from all the 57 parameters was -0.037 and the median of the coefficients from all the 57 parameters was 0.0215. Here, we observe that the stepping ankle flexion angle (1.080) during Step Start (TO - Toe Off) is significant higher than the mean coefficients. The stepping shank flexion angle during Step Start (TO - Toe Off) and Step Stop (HS - Heel Strike) are also quite high (0.996 and 0.908). The knee flexion angle and the hip flexion velocity are also significantly high (0.840 and 0.633). These coefficients suggests that among the original 57 parameters, the above parameters have a stronger significance in determining whether a person would fall or recover during the perturbation. We would utilize these parameters for the time series analysis. The trunk flexion velocity had a high correlation coefficient, but a relatively moderate classification coefficient, however we still use the trunk flexion velocity as a parameter for the time series analysis. The foot flexion has a lower classification coefficient than the rest of the parameters and hence it is ignored in the time series analysis.

Results from Time Series Analysis In this section we observe the results of the time series data for determining the whether the subject has fallen or recovered. The above analysis using correlation and classification helped in narrowing down the parameters for the time series analysis. We ignore the overall kinematic parameters since it had a low classification score. We observe the individual body part kinematic parameter for this analysis since it has an associated angular displacement and velocity which can be then measured using sensors on a device. Out of the 57 parameters that we analyzed, we look into **stepping ankle flexion angle, stepping shank flexion angle, knee flexion angle, hip flexion velocity and trunk flexion velocity** parameters as they had a high correlation and logistic regression coefficient

Table 2.8: Logistic Regression Coefficients for the Individual Body Parts Kinematic Parameters

Parameters	Coefficients
SteppingankleflexTO	1.08011386774
SteppingshankflexTO	0.99606009557
SteppingshankflexHS	0.90861648
SteppingkneeflexHS	0.84030523282464
SteppinghipflexvelHS	0.633115093465
trunkflexvelHS	0.30804390224
SteppingfootflexHS	0.081916362

Table 2.9: Classification Report Using Individual Body Parts Kinematics

Classes	Precision	Recall	F-1
Recovery	0.96	0.96	0.96
Fall	0.88	0.88	0.88

during the above analysis.

Individual trials of a single subject: A typical ankle flexion time series data for a single trial is shown in figure 2.2. The time series data contains the events such as treadmill start, step start and step stop highlighted in red, green and purple vertical lines. It's observed that there is change in the angular displacement at each of the above events. The amount of changes and the corresponding time would help in determining the relevant variables for the time series analysis. A typical shank flexion

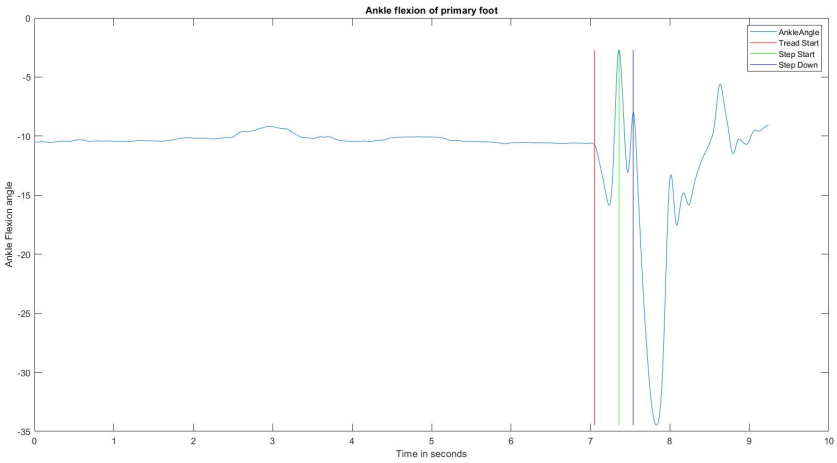

Figure 2.2: Ankle Angle of a Single Subject for a Single Trial

time series data for a single trial is shown in figure 2.3. Here also we observe that there is change in angular displacement at each of the trial events like treadmill start, step start and step stop. A typical knee flexion time series data for a single trial is

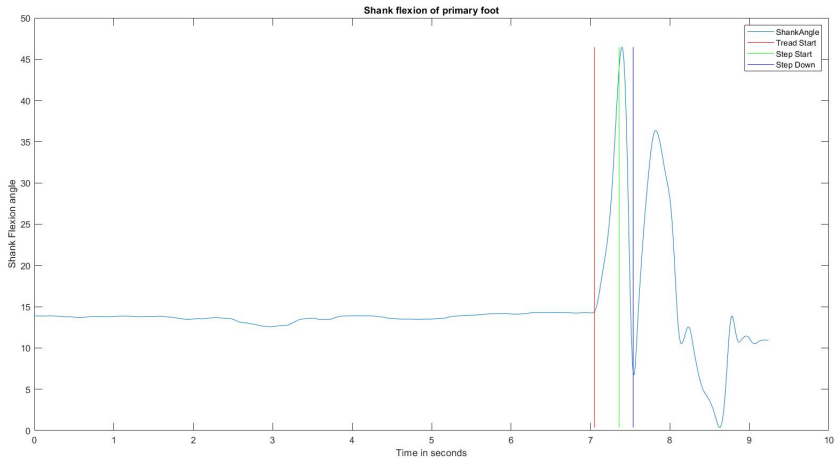

Figure 2.3: Shank Angle of a Single Subject for a Single Trial

shown in figure 2.4. Here also we observe that there is change in angular displacement at each of the trial events like treadmill start, step start and step stop. The

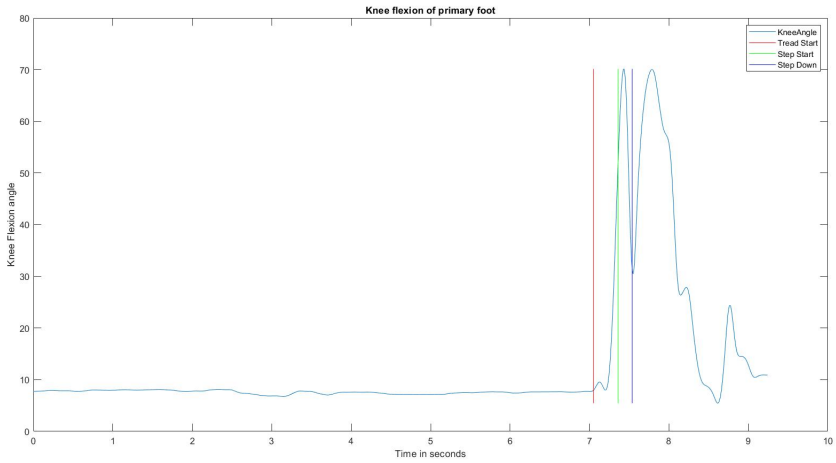

Figure 2.4: Knee Angle of a Single Subject for a Single Trial

velocity plots for the individual trials for a particular subject is not displayed since event times would get lost after the differentiation is performed on the displacement.

Mean plots of fall and recovery for a single subject In this section, we observe the average time series plot for a single subject. The y-axis denotes the angular displacement/velocity and the x-axis denotes % gait cycle. The % gait cycle would be a measure of the time and would be used interchangeably in the discussion. The graphs for both the fall and recoveries are plotted on the same graph (blue for recover and red for fall) to show the difference in the characteristics of the two plots. In figure 2.5 we observe the average for the angular displacement of the ankle. Here it can be observed that the during a fall event the maximum angle is lower than the maximum angle of the recovery event. The time it takes to reach the maximum is faster for recovery than for fall trials. In figure 2.6 we observe the average for the angular displacement of the shank. Here it can be observed that the maximum of the angle is reached much quicker for recovery than for fall. The minimum of the angle is also reached much quicker for recovery than for fall. In figure 2.7 we observe the average for the angular displacement of the knee. Here it can be observed that

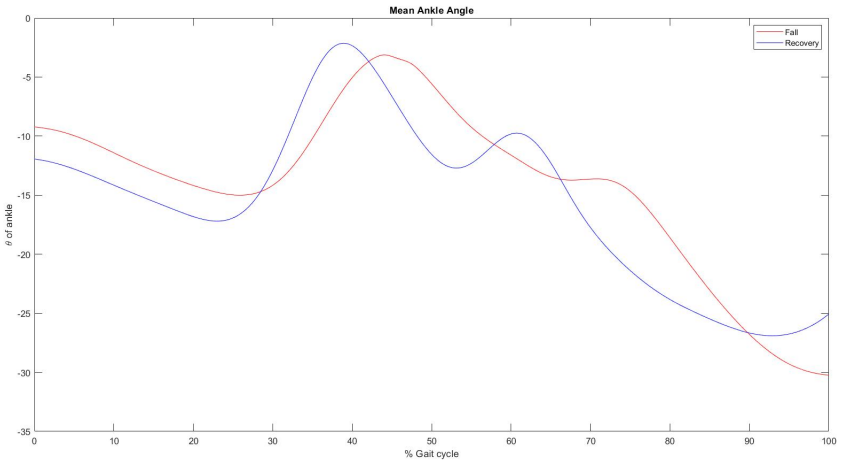

Figure 2.5: Mean Ankle Angle of a Single Subject

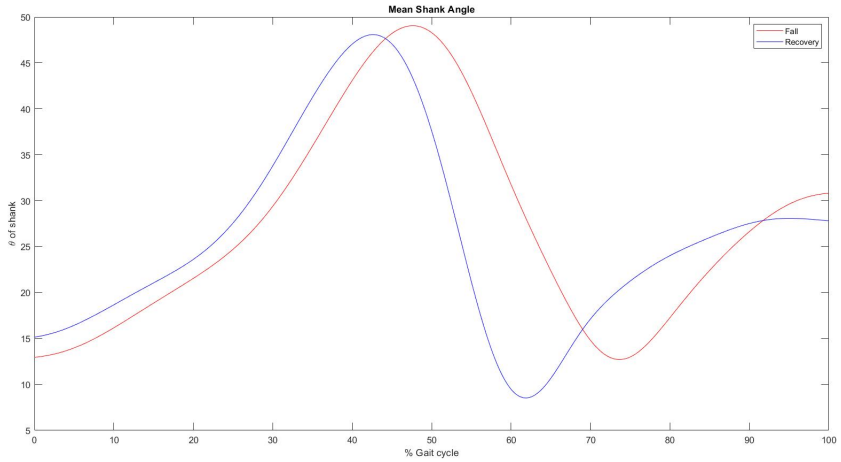

Figure 2.6: Mean Shank Angle of a Single Subject

the maximum of the angle is reached much quicker for recovery than for fall. The minimum of the angle is also reached much quicker for recovery than for fall. The minimum of the angle is also much higher for recovery than for fall. In figure 2.8 we observe the average for the angular velocity of the hip. Here also, it can be observed that the maximum of the velocity is reached much quicker for recovery than for fall. The minimum of the velocity is also reached much quicker for recovery than for fall.

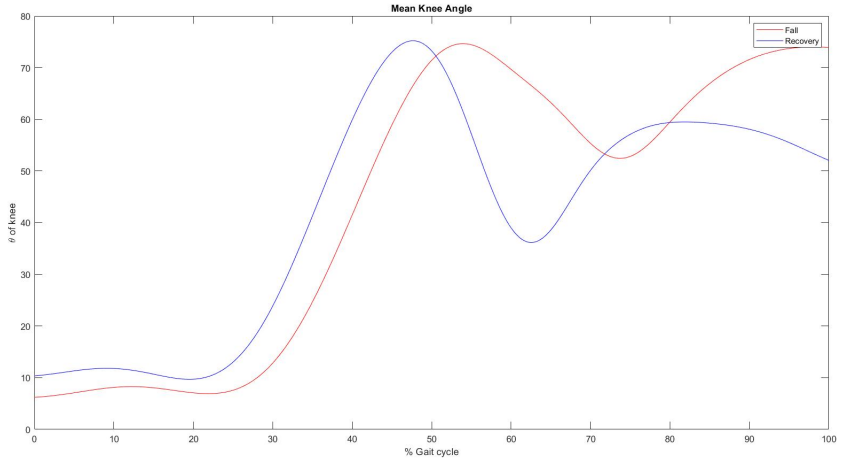

Figure 2.7: Mean Knee Angle of a Single Subject

The minimum of the angle is also much higher for recovery than for fall. In figure

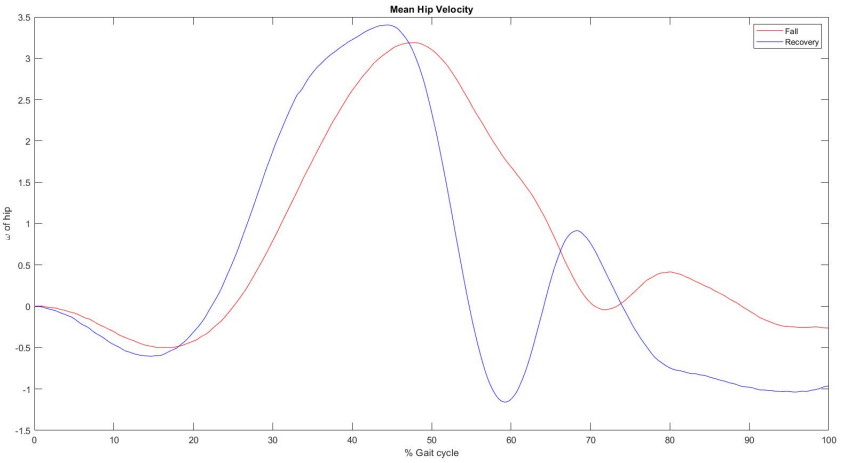

Figure 2.8: Mean Hip Velocity of a Single Subject

2.9 we observe the average for the angular velocity of the trunk. Here also, it can be observed that the maximum velocity is reached much quicker for recovery than for fall. The max velocity is also higher for recovery than for fall. The minimum of the velocity is also reached much quicker for recovery than for fall. The minimum of the

angle is also much higher for recovery than for fall.

Mean plots of fall and recovery for all the subjects In this section we observe

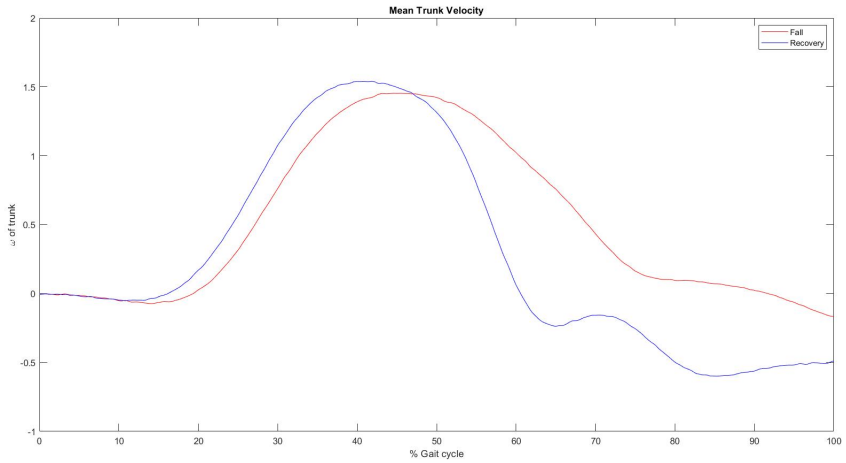

Figure 2.9: Mean Trunk Velocity of a Single Subject

the time series plots averaged for all the subjects and categorized into fall and recovery. In these plots we also display the 95% confidence intervals around the mean plot. The y-axis denotes the angular displacement/velocity and the x-axis denotes the % gait cycle. Here too the % gait cycle is considered a measure of time and will be used interchangeably in the discussion. In figure 2.10 we observe the average ankle angle plots taken for all the subjects. The maximum angle value is higher for recovery than fall in this overall mean plots. It suggests that the subject would more likely recover if their highest ankle angular displacement is above a certain threshold. The ankle angular displacement corresponds to the plantar flexion angle during push off. In figure 2.11 we observe the average shank angle plots taken for all the subjects. As observed with the mean plots of individual subjects, The maximum angle is reached faster for recovery than for fall. The maximum angle value is also higher for recovery than fall in this overall mean plots. As with the individual mean plots the minimum of the angle is much higher for recovery than fall. From the observations, it suggests

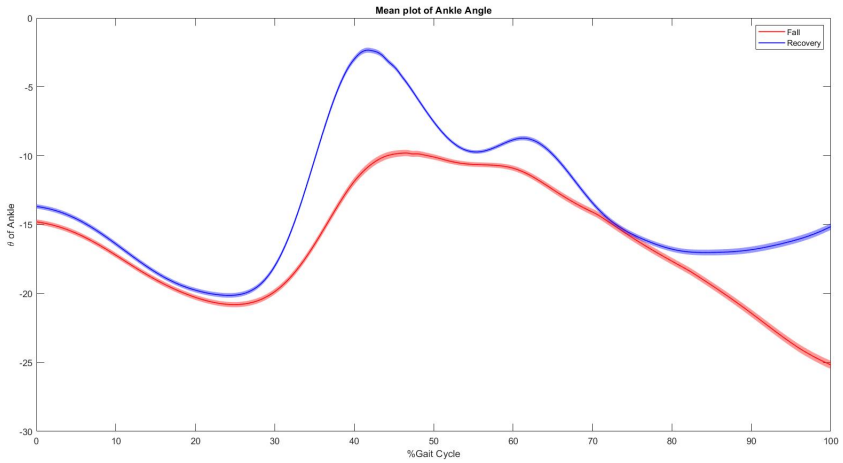

Figure 2.10: Mean Ankle Angle of All Subjects

that the subject would more likely recover if they are able to reach their highest shank angular displacement faster. In figure 2.12 we observe the average knee angle plots

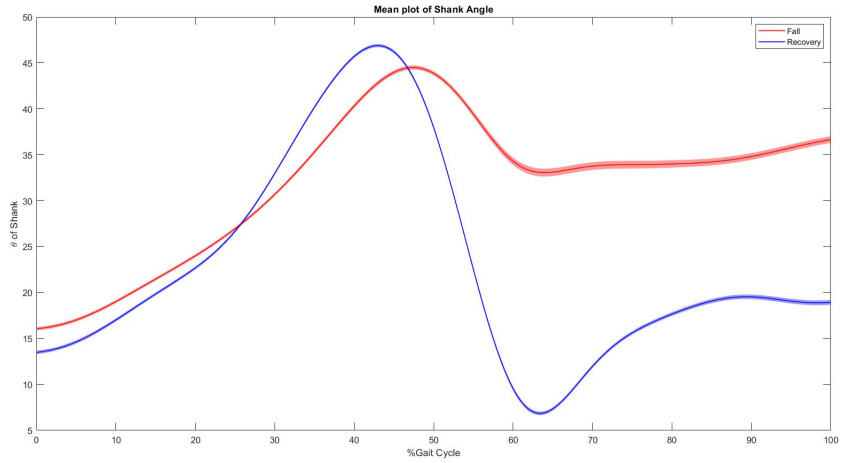

Figure 2.11: Mean Shank Angle of All Subjects

taken for all the subjects. As observed with the mean plots of individual subjects, The maximum angle is reached faster for recovery than for fall. The maximum angle value is also higher for recovery than fall in this overall mean plots. As with the individual

mean plots the minimum of the angle is much higher for recovery than fall. From the observations, it suggests that the subject would more likely recover if they are able to reach their highest knee angular displacement faster. In figure 2.13 we observe the

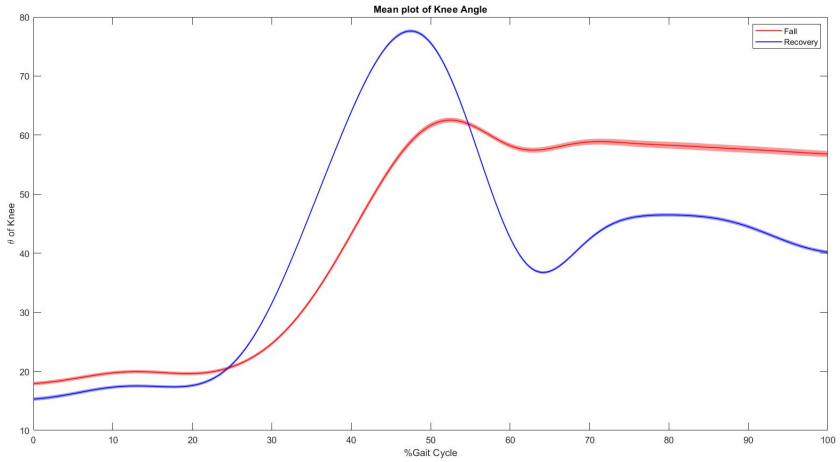

Figure 2.12: Mean Knee Angle of All Subjects

average hip velocity plots taken for all the subjects. As observed with the mean plots of individual subjects, the maximum velocity value is higher for recovery than fall in this overall mean plots. As with the individual mean plots the minimum of the angle is much higher for recovery than fall. From the observations, it suggests that the subject would more likely recover if they are able to reach a certain velocity in their stepping hip. In figure 2.14 we observe the average trunk velocity plots taken for all the subjects. As observed with the mean plots of individual subjects, the maximum velocity value is higher for recovery than fall in this overall mean plots. As with the individual mean plots the minimum of the angle is much higher for recovery than fall. The trunk velocity falls of to the minimum after the maximum is reached much quicker for recovery than fall. From the observations, it suggests that the subject would more likely recover if they are able to quickly reduce their trunk velocity.

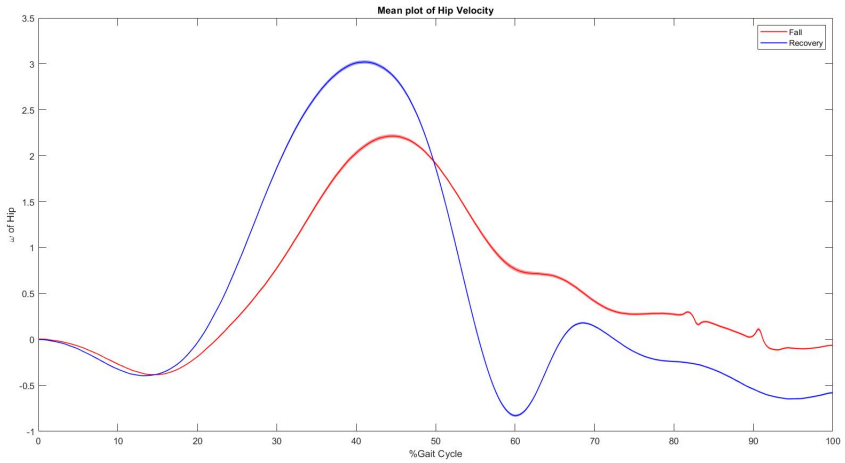

Figure 2.13: Mean Hip Velocity of All Subjects

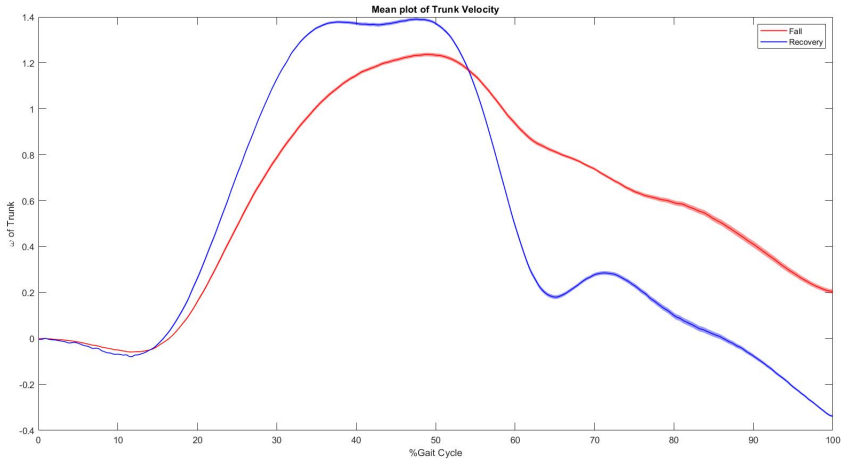

Figure 2.14: Mean Trunk Velocity of All Subjects

The variables obtained from table 2.3 for the shank and trunk is given in the table 2.10 and 2.11. It can be observed from the shank statistics that the average Max Angle is greater for falls than recovery, the average Max Angle time is slower for fall and recovery. It's significant that the subjects is likely to recover if they reach max peak before 50% of the gait cycle. The Maximum and Minimum Velocity, Rise velocity time and Fall velocity time shows that the subjects who are able to

reach higher velocity in shank movement can recover from the perturbations better. It can be observed from the trunk statistics that the Maximum Angle is higher for falls than recovery, which suggests that if the trunk gets deflected too much, then subject is more likely to fall. The Maximum and Minimum Velocity are higher for falls than recoveries which suggests that the faster the trunk is controlled during the perturbation, the better the subject can recover. The Rise velocity time is higher for fall than for recovery which suggests that the subjects whose trunk velocity increases rapidly (less control of trunk) will more like fall during a perturbation.

Table 2.10: Statistics of the Time Series Data for Shank

Variables	Mean Fall	Mean Recovery
Max Angle (θ)	35.272	30.288
Max Angle Time (%gait)	**62.857**	**42.86**
Max Velocity (θ/sec)	1.104	2.249
Max Velocity Time	39.192	42.09
Min Velocity (θ/sec)	2.982	4.696
Min Velocity Time (%gait)	66.981	64.39
Rise velocity time (%gait)	**39.182**	**28.92**
Fall velocity time (%gait)	**27.789**	**22.30**

2.3.1 Discussion

The time-series analysis of the individual subjects and the average plots of all the subjects highlights some important features of the parameter we extracted from the correlation and classification analysis. The **hypothesis** as previously stated is to

Table 2.11: Statistics of the Time Series Data for Trunk

Variables	Mean Fall	Mean Recovery
Max Angle (θ)	**57.599**	**50.948**
Max Angle Time (%gait)	91.88	79.50
Max Velocity (θ/sec)	1.411	1.608
Max Velocity Time	48.92	39.63
Min Velocity (θ/sec)	1.459	2.061
Min Velocity Time (%gait)	97.72	94.45
Rise velocity time (%gait)	**36.41**	**28.27**
Fall velocity time (%gait)	**48.81**	**54.82**

determine the kinematic parameters that firstly, can be measured using IMU sensors placed on the body similar to designs mentioned in chapter 1 and secondly, these parameters will be sufficient to distinguish between a fall and recovery.

As observed from the results above, the **ankle angular displacement** is inconclusive in determining whether the person would fall or recover since in the individual plots the time to reach max peak is faster in recovery than fall, but the same is not reflected in the average of the overall ankle angle plots. The **knee angular displacement** for the overall average plots suggests that the maximum angle for recovery is higher than the maximum angle for a fall but the same is not reflected in the individual averages and hence this feature will not be reliable in distinguishing between a fall and recovery. The **hip velocity** is a good measure since for both the individual averages and the overall average it reaches its max peak faster for recovery than fall. However, for the thesis we will be ignoring the hip velocity since the objective of the analysis is

to find out the minimum parameters and we would require two sensors to distinguish between the stepping hip and the base hip. The **shank angular displacement** and **trunk angular velocity** are the measures which significantly determines whether a subject has fallen or recovered. In both the measures, the individual averages and the overall averages of the rise time to the maximum peak were much faster for recoveries than for falls. The observations suggest that the subjects who can move their shank faster and reach a certain maximum angular displacement are able to reduce the chances of falling. The results also suggest that the subjects who can reduce the trunk velocity faster are able to recover.

2.4 Conclusions

In chapter 2, the analysis of the treadmill perturbation data is shown. We observe the three different categories of the data (i.e. overall kinematics, kinematics of individual body parts, and kinetics). Techniques such as correlation and logistics regressions were used to determine the parameters which will be most helpful in detecting the falls when a subject encounters perturbations like ones provided for the data collection. The parameters like stepping ankle flexion angle, stepping shank flexion angle, hip flexion velocity, and trunk flexion velocity were found to be the most significant parameters for distinguishing from falls and recovery. The time-series data of these parameters were analyzed. It was found from the time-series data that the subjects who for particular trials moved their shank faster and reached a certain maximum in the shank angular displacement were able to recover from the perturbations. Its also observed that the subjects who were able to reduce the trunk velocity faster were also able to recover in those trials.

2.4.1 Summary of the Results From Chapter 1 and 2

In chapter 1, the design of an unobtrusive, cost-effective easy to wear Active Ankle-Foot Orthosis which uses a pneumatic double active cylinder to supplement the ankle in both plantar flexion and dorsiflexion. The device described is capable of housing a powered remote air supply and displaces the majority of the heavier components to the torso of the users keeping the additional weight of the ankle lighter than comparative designs. The results from the preliminary tests conducted showed that the device was able to increase the **anterior-posterior ground reaction force** of the 4 subjects. To achieve this result a custom control algorithm utilizing timing and angle parameters was utilized to determine the various phases of the gait cycle. The results from chapter 2 suggest that the **shank angular displacement** and the **trunk angular velocity** are parameters which if measured using wearable IMU sensors can potentially detect whether a user is going to fall early enough for the device to actuate and prevent the fall. These two parameters are easy to measure and can integrate well with the design of the AAFO mentioned in chapter 1. In chapter 1, the IMU sensors were already used on the shank to determine the difference of the angular displacement between the two legs and was a control parameter to actuate the pneumatic cylinders. The results from chapter 2 suggest that instead of using the difference of angular displacement, a threshold of the angular displacement of a particular leg can be utilized. It is seen from the results that when the maximum peak of the angular displacement is reached after 50% of the gait cycle, then the person is most likely to fall and actuation of the device is required to provide a sufficient ground reaction force (push-off) that can aid the recovery of the person. The timing parameters t_1 and t_2 as mentioned in the control algorithm 1 can be used to determine the % gait cycle of the step. Additionally, an IMU sensor can be placed on the trunk

to determine whether the actuation of the second leg is required or not. The above results in chapter 2 suggest that the velocity of the trunk needs to be reduced quickly enough to facilitate recovery. The threshold for the angular velocity of the trunk can be incorporated in the control algorithm 1 mention in chapter 1 to determine if the additional actuation is required or not.

2.4.2 Future Directions

Future studies can utilize the results from both chapters 1 and 2 to improve the design and generate more decisive control parameters for actuation. Although, the preliminary test conducted in chapter 1 showed the improvement of ground reaction force on the subjects, more thorough and detailed testing of the device is necessary for better reliability in a real-world setting. A more detailed clinical study of the device in the future would include testing the device on more number of subjects. A more detailed analysis can be performed on the ground reaction force results to state with a statistical level of certainty that the device is capable of increasing propulsion during push-off. The current design aims to reduce the weight on the ankle by attaching the majority of the heavier components on the torso of the users. However, the weight can be further reduced by using plastic-based or carbon fiber-based double-acting cylinders instead of metal ones. Even lighter materials can be used for 3D printing the custom ankle brace. In future testing of the device, a metabolic cost study can be performed to determine whether the device saves the overall metabolic cost of walking. The results from chapter 2 can be utilized in the control algorithm in chapter 1 to test if there is an improvement of device performance by incorporating the timing and angle parameters from the data analysis. Chapter 2 shortlists the kinematic parameters using correlation analysis and logistic regression. In the future, additional statistical analysis like Linear Discriminant Analysis (LDA) or Principal

Component Analysis (PCA) can be performed to determine these parameters with a higher degree of certainty. Modern statistical prediction models like Recurrent Neural Networks (RNNs) or Long-Short Term Memory (LSTM) can be utilized in the future to utilize the time series data for a better prediction of falls and recoveries.

URL https://www.cdc.gov/stroke/facts.htm (2020).

Adafruit, "Adafruit 9-dof absolute orientation imu fusion breakout - bno055", URL https://www.adafruit.com/product/2472 (2020).

Alam, M., I. A. Choudhury and A. Bin Mamat, "Mechanism and design analysis of articulated ankle foot orthoses for drop-foot.", TheScientificWorldJournal **2014**, 867869, URL http://search.proquest.com/docview/1544323599/ (2014).

Alwan, M., P. Rajendran, S. Kell, D. Mack, S. Dalal, M. Wolfe and R. Felder, "A smart and passive floor-vibration based fall detector for elderly", in "2006 2nd International Conference on Information & Communication Technologies", vol. 1, pp. 1003–1007 (IEEE, 2006).

Batchelor, F. A., S. F. Mackintosh, C. M. Said and K. D. Hill, "Falls after stroke", International Journal of Stroke **7**, 6, 482–490, URL https://doi.org/10.1111/j.1747-4949.2012.00796.x, pMID: 22494388 (2012).

Boehler, A., K. Hollander, T. Sugar and D. Shin, "Design, implementation and test results of a robust control method for a powered ankle foot orthosis (afo)", in "2008 IEEE International Conference on Robotics and Automation", pp. 2025–2030 (IEEE, 2008).

Burns, E. and R. Kakara, "Deaths from falls among persons aged ¿65 years - united states, 2007–2016", URL https://www.cdc.gov/mmwr/volumes/67/wr/mm6718a1.htm (2018).

Chander, H., R. F. Burch, P. Talegaonkar, D. Saucier, T. Luczak, J. E. Ball, A. Turner, S. N. K. Kodithuwakku Arachchige, W. Carroll, B. K. Smith, A. Knight and R. K. Prabhu, "Wearable stretch sensors for human movement monitoring and fall detection in ergonomics.", International journal of environmental research and public health **17**, 10, URL http://search.proquest.com/docview/2406310107/ (2020).

Chaudhuri, S., "Examining the feasibility and acceptability of a fall detection device", URL http://search.proquest.com/docview/1675024998/ (2015).

Chen, J., K. Kwong, D. Chang, J. Luk and R. Bajcsy, "Wearable sensors for reliable fall detection", in "2005 IEEE Engineering in Medicine and Biology 27th Annual Conference", pp. 3551–3554 (2005).

Crenshaw, J. R. and M. D. Grabiner, "The influence of age on the thresholds of compensatory stepping and dynamic stability maintenance", Gait & Posture **40**, 3, 363–368 (2014).

Dennis, M., S., K. Lo, M., M. Mcdowall, M. and T. West, M., "Fractures after stroke: Frequency, types, and associations", Stroke: Journal of the American Heart Association **33**, 3, 728–734 (2002).

Ferris, D. P., J. M. Czerniecki and B. Hannaford, "An ankle-foot orthosis powered by artificial pneumatic muscles.", Journal of applied biomechanics **21**, 2, 189–197, URL `http://search.proquest.com/docview/68446714/` (2005).

Ferris, D. P., K. E. Gordon, G. S. Sawicki and A. Peethambaran, "An improved powered ankle–foot orthosis using proportional myoelectric control", Gait & Posture **23**, 4, 425–428 (2006).

Francis, C. A., A. L. Lenz, R. L. Lenhart and D. G. Thelen, "The modulation of forward propulsion, vertical support, and center of pressure by the plantarflexors during human walking", Gait & Posture **38**, 4, 993–997 (2013).

Geurts, A. C., M. de Haart, I. J. van Nes and J. Duysens, "A review of standing balance recovery from stroke", Gait & Posture **22**, 3, 267–281 (2005).

Goutte, C. and É. Gaussier, "A probabilistic interpretation of precision, recall and f-score, with implication for evaluation", in "ECIR", (2005).

Hatem, S. M., G. Saussez, M. D. Faille, V. Prist, X. Zhang, D. Dispa and Y. Bleyenheuft, "Rehabilitation of motor function after stroke: a multiple systematic review focused on techniques to stimulate upper extremity recovery", Frontiers in Human Neuroscience **10**, 2016, URL `https://doaj.org/article/21f0872ab10b496b99166baffd640dcd` (2016).

Herndon, J. G., C. G. Helmick, R. W. Sattin, J. A. Stevens, C. Devito and P. A. Wingo, "Chronic medical conditions and risk of fall injury events at home in older adults", Journal of the American Geriatrics Society **45**, 6, 739–743 (1997).

Honeycutt, C. F., M. Nevisipour and M. D. Grabiner, "Characteristics and adaptive strategies linked with falls in stroke survivors from analysis of laboratory-induced falls", Journal of Biomechanics **49**, 14, 3313–3319 (2016).

Hwang, S., J. Kim, J. Yi, K. Tae, K. Ryu and Y. Kim, "Development of an active ankle foot orthosis for the prevention of foot drop and toe drag", in "2006 International Conference on Biomedical and Pharmaceutical Engineering", pp. 418–423 (2006).

Jensen, J. L., L. A. Brown and M. H. Woollacott, "Compensatory stepping: The biomechanics of a preferred response among older adults", Experimental Aging Research **27**, 4, 361–376, URL `http://www.tandfonline.com/doi/abs/10.1080/03610730109342354` (2001).

Jørgensen, L., K., T. Engstad, K. and B. Jacobsen, K., "Higher incidence of falls in long-term stroke survivors than in population controls: Depressive symptoms predict falls after stroke", Stroke: Journal of the American Heart Association **33**, 2, 542–547 (2002).

Kadaba, M. P., H. K. Ramakrishnan and M. E. Wootten, "Measurement of lower extremity kinematics during level walking", J. Orthop. Res. **8**, 3, 383–392 (1990).

Kawamura, S., T. Yamamoto, D. Ishida, T. Ogata, Y. Nakayama, O. Tabata and S. Sugiyama, "Development of passive elements with variable mechanical impedance for wearable robots", vol. 1, pp. 248–253 (2002).

Kluding, P., M., K. Dunning, W., M. O'dell, S., S. Wu, S., J. Ginosian, S., J. Feld, S. and K. Mcbride, S., "Foot drop stimulation versus ankle foot orthosis after stroke: 30-week outcomes", Stroke **44**, 6, 1660–1669 (2013).

Li, Y., K. C. Ho and M. Popescu, "A microphone array system for automatic fall detection", IEEE Transactions on Biomedical Engineering **59**, 5, 1291–1301 (2012).

Light, J., S. Cha and M. Chowdhury, "Optimizing pressure sensor array data for a smart-shoe fall monitoring system", in "2015 IEEE SENSORS", pp. 1–4 (2015).

McCullagh, P., *Generalized linear models*, Monographs on statistics and applied probability ; 37 (Chapman and Hall, 1989), 2nd ed.. edn.

Mcilroy, W. and B. Maki, "Task constraints on foot movement and the incidence of compensatory stepping following perturbation of upright stance", Brain Research **616**, 1-2, 30–38 (1993).

Mukaka, M. M., "Statistics corner: A guide to appropriate use of correlation coefficient in medical research.", Malawi medical journal : the journal of Medical Association of Malawi **24**, 3, 69–71, URL `http://search.proquest.com/docview/1348500849/` (2012).

Mukhopadhyay, S. C., "Wearable sensors for human activity monitoring: A review", IEEE Sensors Journal **15**, 3, 1321–1330 (2015).

Nevisipour, M., *Evaluating the Effects of Ankle-Foot-Orthoses, Functional Electrical Stimulators, and Trip-specific Training on Fall Outcomes in Individuals with Stroke* (2019).

Nevisipour, M. and C. F. Honeycutt, "The impact of ankle-foot-orthosis (afo) use on the compensatory stepping response required to avoid a fall during trip-like perturbations in young adults: Implications for afo prescription and design", Journal of Biomechanics **103**, 109703 (2020).

Owings, T. M., M. J. Pavol and M. D. Grabiner, "Mechanisms of failed recovery following postural perturbations on a motorized treadmill mimic those associated with an actual forward trip", Clinical Biomechanics **16**, 9, 813–819 (2001).

Palmer, M. L., "Sagittal plane characterization of normal human ankle function across a range of walking gait speeds", (2002).

Pouwels, S., A. Lalmohamed, B. Leufkens, A. De Boer, C. Cooper, T. Van Staa and F. De Vries, "Risk of hip/femur fracture after stroke: A population-based case-control study", Stroke **40**, 10, 3281–3285 (2009).

Qi, H., G. M. Bone and Y. Zhang, "Position control of pneumatic actuators using three-mode discrete-valued model predictive control", Actuators **8**, 3, 56, URL https://doaj.org/article/55049024713e4eb3a1aa5ab86f8d51ff (2019).

Quintero, D., D. J. Lambert, D. J. Villarreal and R. D. Gregg, "Real-time continuous gait phase and speed estimation from a single sensor", in "2017 IEEE Conference on Control Technology and Applications (CCTA)", vol. 2017, pp. 847–852 (IEEE, 2017).

Ramnemark, A., L. Nyberg, B. Borssén, T. Olsson and Y. Gustafson, "Fractures after stroke", Osteoporosis International **8**, 1, 92–95 (1998).

Shany, T., S. J. Redmond, M. R. Narayanan and N. H. Lovell, "Sensors-based wearable systems for monitoring of human movement and falls", IEEE Sensors Journal **12**, 3, 658–670 (2012).

Shung, K. P., "Accuracy, precision, recall or f1?", URL https://towardsdatascience.com/accuracy-precision-recall-or-f1-331fb37c5cb9 (2018).

Simons, C. D., E. H. van Asseldonk, H. v. D. Kooij, A. C. Geurts and J. H. Buurke, "Ankle-foot orthoses in stroke: Effects on functional balance, weight-bearing asymmetry and the contribution of each lower limb to balance control", Clinical Biomechanics **24**, 9, 769–775 (2009).

Sixsmith, A. and N. Johnson, "A smart sensor to detect the falls of the elderly", IEEE Pervasive Computing **3**, 2, 42–47 (2004).

Taborri, J., E. Palermo, S. Rossi and P. Cappa, "Gait partitioning methods: A systematic review", Sensors **16**, 1, 66, URL http://search.proquest.com/docview/1764191779/ (2016).

Wade, D. T., V. A. Wood and R. L. Hewer, "Recovery after stroke–the first 3 months.", Journal of Neurology, Neurosurgery & Psychiatry **48**, 1, 7–13, URL http://jnnp.bmj.com/content/48/1/7.full.pdf (1985).

Wåhlin, N. and L. Wrange, "Development of techniques for measuring the mobility of knee joints in children with cerebral palsy", (2018).

Watanabe, T., H. Saito, E. Koike and K. Nitta, "A preliminary test of measurement of joint angles and stride length with wireless inertial sensors for wearable gait evaluation system", Computational Intelligence and Neuroscience **2011**, 2011, 411–422 (2011).

Weerdesteyn, V., M. de Niet, H. van Duijnhoven and A. Geurts, "Falls in individuals with stroke", Journal Of Rehabilitation Research And Development **45**, 8, 1195–1213 (2008).

Yamamoto, S., M. Ebina, S. Miyazaki, H. Kawai and T. Kubota, "Development of a new ankle-foot orthosis with dorsiflexion assist, part 1: Desirable characteristics of ankle-foot orthoses for hemiplegic patients", Journal of Prosthetics and Orthotics **9**, 4, 174–179 (1997).

Yarkony, G. and V. Sahgal, "Contractures. a major complication of craniocerebral trauma", Clinical Orthopaedics and Related Research **219**, 93–96 (1987).

APPENDIX A

ARDUINO CODE FOR DEVICE OPERATION

The following code was written in Arduino IDE and was used for the device operation.

```
#include <Wire.h>
#include <Adafruit_Sensor.h>
#include <Adafruit_BNO055.h>
#include <utility/imumaths.h>
#include <EEPROM.h>
#include <ESP8266WiFi.h>
#include<WiFiClient.h>
#include<ESP8266WebServer.h>

uint16_t BNO055_SAMPLERATE_DELAY_MS = 150;
int x = 1;
double offset1;
double offset2;
double offset3;
#define TCAADDR 0x70

//Declare the sensor variables
Adafruit_BNO055 bno1 = Adafruit_BNO055(55);
Adafruit_BNO055 bno2 = Adafruit_BNO055(56);
Adafruit_BNO055 bno3 = Adafruit_BNO055(57);
//Declare Server setup
const char* ssid = "RayWifiDaq";
const char* password = "sambarta4444";
WiFiServer server(80);

/*Select the Multiplexer output*/
void tcaselect(uint8_t i) {
  if (i > 7) return;

  Wire.beginTransmission(TCAADDR);
  Wire.write(1 << i);
  Wire.endTransmission();
}

void setup(void)
{
  //Sensor Setup
  Serial.begin(9600);

  Serial.println("Orientation Sensor Test"); Serial.println("
     ");

  /* Initialise the 1st sensor */
```

```
tcaselect(2);  // select port 2
bno1.begin();
/* Initialise the 1st sensor */

tcaselect(3);  // select port 3
bno2.begin();
/* Initialise the 1st sensor */

tcaselect(4);  // select port 4
bno3.begin();
tcaselect(2);
initialize1stSensor(bno1);
delay(500);
tcaselect(3);
initialize2ndSensor(bno2);
delay(500);
tcaselect(4);
initialize3rdSensor(bno3);
delay(500);

//Calibrate 1st Sensor
tcaselect(2);
calibrate1stSensor(bno1);
Serial.println("Sensor 1 calibrated");
//Calibrate 2nd Sensor
tcaselect(3);
calibrate2ndSensor(bno2);
//Set crystal use for both sensors
Serial.println("Sensor 2 calibrated");

bno1.setExtCrystalUse(true);
bno2.setExtCrystalUse(true);
bno3.setExtCrystalUse(true);

//Wifi Setup
Serial.printf("Connecting to %s ", ssid);
WiFi.begin(ssid, password);
while (WiFi.status() != WL_CONNECTED)
{
  delay(500);
  Serial.print(".");
}
Serial.println(" connected");
server.begin();
Serial.println("IP address");
Serial.print(WiFi.localIP());
/*Set pin mode for output*/
```

```
  pinMode(12, OUTPUT);
  pinMode(14, OUTPUT);
  pinMode(13, OUTPUT);
  pinMode(15, OUTPUT);
  pinMode(0, OUTPUT);
}
void loop(void)
{
  //  counterLeft = 0;
  //  counterRight = 0;
  //  int Lcounter;
  //  int Rcounter;
  int leg = 0;
  int counter = 0;
  WiFiClient client = server.available();
  if (client) {
    Serial.println("\nClient Connected\n");
    //client.println("Connected to feather BNO055");
    /*Check client connection*/
    while (client.connected()) {
      //Serial.println("Client in while");//for debug only
      if (client.available()) {
        /*Take input from user*/
        char inp = client.read();
        /*Setup calibration for sensors*/
        /*Read sensor value*/
        //Serial.println("Reading sensor"); //for debug only
        tcaselect(2);
        imu::Vector<3> euler1 = bno1.getVector(
            Adafruit_BNO055::VECTOR_EULER);
        imu::Vector<3> angVel1 = bno1.getVector(
            Adafruit_BNO055::VECTOR_GYROSCOPE);
        tcaselect(3);
        imu::Vector<3> euler2 = bno2.getVector(
            Adafruit_BNO055::VECTOR_EULER);
        imu::Vector<3> angVel2 = bno2.getVector(
            Adafruit_BNO055::VECTOR_GYROSCOPE);
        tcaselect(4);
        imu::Vector<3> euler3 = bno3.getVector(
            Adafruit_BNO055::VECTOR_EULER);
        imu::Vector<3> angVel3 = bno3.getVector(
            Adafruit_BNO055::VECTOR_GYROSCOPE);
        if (x == 1) {
          offset1 = 90 - euler1.y();
          offset2 = 90 - euler2.y();
          offset3 = 100 - euler3.y();
          x = 2;
```

```
        }

        /*Write sensor value*/
        String msg = String(euler1.y() + offset1) + "\t" +
           String(angVel1.y()) + "\t" + String(euler2.y() +
           offset2) + "\t" + String(angVel2.y()) + "\t" +
           String(euler3.y() + offset3) + "\t" + String(
           angVel3.y());

        //Serial.println(msg);
        client.println(msg);
//        Serial.print(abs((euler1.y() + offset1) - (euler2.y
   () + offset2)));
        if (counter <= 0) {
          if (abs((euler1.y() + offset1) - (euler2.y() +
             offset2)) >= 9.5) {
            if ((euler1.y() + offset1) < (euler2.y() +
               offset2) && leg != 1) {
              counter = 2;
              leg = 1;
//              Serial.print("left step");
              digitalWrite(13, HIGH);
              digitalWrite(15, LOW);
              digitalWrite(14, LOW);
              digitalWrite(12, LOW);
            } else if((euler1.y() + offset1) > (euler2.y() +
               offset2) && leg != 2){
              counter = 3;
              leg = 2;
//              Serial.print("right step");
              digitalWrite(13, LOW);
              digitalWrite(15, LOW);
              digitalWrite(14, HIGH);
              digitalWrite(12, LOW);
            }
          } else {
//            Serial.print("still");
            leg = 0;
            digitalWrite(13, LOW);
            digitalWrite(15, LOW);
            digitalWrite(14, LOW);
            digitalWrite(12, LOW);
          }

        }
        counter--;
        if (counter < 1) {
```

```
            if (leg == 1) {
//              Serial.print("left return");
              digitalWrite(13, LOW);
              digitalWrite(15, HIGH);
              digitalWrite(14, LOW);
              digitalWrite(12, LOW);

            } else if(leg == 2){
//              Serial.print("right return");
              digitalWrite(13, LOW);
              digitalWrite(15, LOW);
              digitalWrite(14, LOW);
              digitalWrite(12, HIGH);
            }

          }


          delay(BNO055_SAMPLERATE_DELAY_MS);
        }
      }
    }
    //  tcaselect(0);
    //  imu::Vector<3> euler1 = bno1.getVector(Adafruit_BNO055
        ::VECTOR_EULER);
    //  tcaselect(1);
    //  imu::Vector<3> euler2 = bno2.getVector(Adafruit_BNO055
        ::VECTOR_EULER);
    //  //String msg = String(euler1.x())+"\t"+String(euler1.y
        ())+"\t"+String(euler1.z());
    //  String msg1 = String(String(euler1.y()));
    //  Serial.println("\n 1st Sensor");
    //  Serial.println(msg1);
    //  //String msg2 = String(euler2.x())+"\t"+String(euler2.y
        ())+"\t"+String(euler2.z());
    //  String msg2 = String(String(euler2.y()));
    //  Serial.println("\n 2nd Sensor");
    //  Serial.println(msg2);
    //
    //  delay(BNO055_SAMPLERATE_DELAY_MS);
}

void initialize1stSensor(Adafruit_BNO055 bno) {
  tcaselect(2);
  if (!bno.begin())
  {
    /* There was a problem detecting the BNO055 ... check
```

```
      your connections */
    Serial.print("Ooops, no BNO055 detected ... Check your
      wiring or I2C ADDR!");
    while (1);
  } else {
    Serial.println("#1 is working");
  }
}
void initialize2ndSensor(Adafruit_BNO055 bno) {
  tcaselect(3);
  if (!bno.begin())
  {
    /* There was a problem detecting the BNO055 ... check
      your connections */
    Serial.print("Ooops, no BNO055 detected ... Check your
      wiring or I2C ADDR!");
    while (1);
  } else {
    Serial.println("#2 is working");
  }
}
void initialize3rdSensor(Adafruit_BNO055 bno) {
  tcaselect(4);
  if (!bno.begin())
  {
    /* There was a problem detecting the BNO055 ... check
      your connections */
    Serial.print("Ooops, no BNO055 detected ... Check your
      wiring or I2C ADDR!");
    while (1);
  } else {
    Serial.println("#3 is working");
  }
}

void calibrate1stSensor(Adafruit_BNO055 bno) {
  Serial.println("Calibrating sensor 1 \n");
  adafruit_bno055_offsets_t calibData1;
  calibData1.accel_offset_x = 4;
  calibData1.accel_offset_y = -207;
  calibData1.accel_offset_z = 31;
  calibData1.gyro_offset_x = -1;
  calibData1.gyro_offset_y = -1;
  calibData1.gyro_offset_z = -1;
  calibData1.mag_offset_x = -203;
  calibData1.mag_offset_y = -162;
  calibData1.mag_offset_z = -160;
```

```
  calibData1.accel_radius = 1000;
  calibData1.mag_radius = 606;
  bno.setSensorOffsets(calibData1);
  Serial.println("\n Sensor 1 calibrated \n");
}

void calibrate2ndSensor(Adafruit_BNO055 bno) {
  Serial.println("Calibrating sensor 1 \n");
  adafruit_bno055_offsets_t calibData1;
  calibData1.accel_offset_x = -10;
  calibData1.accel_offset_y = -86;
  calibData1.accel_offset_z = 12;
  calibData1.gyro_offset_x = -1;
  calibData1.gyro_offset_y = -2;
  calibData1.gyro_offset_z = -1;
  calibData1.mag_offset_x = -318;
  calibData1.mag_offset_y = 77;
  calibData1.mag_offset_z = -142;
  calibData1.accel_radius = 1000;
  calibData1.mag_radius = 709;
  bno.setSensorOffsets(calibData1);
  Serial.println("\n Sensor 1 calibrated \n");
}

void checkCalibrationStatus(Adafruit_BNO055 bno, WiFiClient
   client) {
  if (!bno.isFullyCalibrated()) {
    client.println("sensor1 not fully calibrated");
  } else {
    client.println("sensor1 calibrated");
  }
}
```

APPENDIX B

MATLAB CODE FOR DATA ANALYSIS

The following code was written in MATLAB and was used for data analysis

```
%Code for analyzing the Joint Angle Data
clc;
clear all;
close all;
%% Extract and Read files
%data_directory = uigetdir('','Select Joint Angle Directory')
    ;
%Get joint angle
[jointAngleFile, jointAngleFilePath] = uigetfile({'*.txt'},'
    Select joint angle file for a trial');

[eventFile,eventFilePath] = uigetfile({'*.xlsx';'*.xls'},'
    Select the excel file for reading the data'); %Select the
    excel file from the folder
[eventData, eventText] = xlsread(fullfile(eventFilePath ,
    eventFile)); %Read the excel file and save it as a
    variable in workspace

f1 =fopen(fullfile(jointAngleFilePath,jointAngleFile));
[data,count] = fscanf(f1,'%f',[67,Inf]);
data = data';



%% Process files and headers for the extracted data

% Set the headers from the original get joint angle
    processing file

column_headers = {'Rknee_flexion','Rknee_adduction','
    Rknee_exrotation','Lknee_flexion','Lknee_adduction','
    Lknee_exrotation',...
                'Rshank_flexion','Rshank_adduction','
                    Rshank_exrotation','Lshank_flexion','
                    Lshank_adduction','Lshank_exrotation',...
                'Rhip_flexion','Rhip_adduction','
                    Rhip_exrotation','Lhip_flexion','
                    Lhip_adduction','Lhip_exrotation',...
                'pelvis_forwardtilt','pelvis_righttilt','
                    pelvis_rightrotation','trunk_flexion','
                    trunk_righttilt','trunk_rightrotation',...
                'head_flexion','head_righttilt','
                    head_rightrotation','neck_flexion','
                    neck_righttilt','neck_rightrotation',...
                'Rankle_flexion','Rankle_adduction','
```

```
                    Rankle_exrotation','Lankle_flexion','
                    Lankle_adduction','Lankle_exrotation',...
                'Rfoot_flexion','Rfoot_adduction','
                    Rfoot_exrotation','Lfoot_flexion','
                    Lfoot_adduction','Lfoot_exrotation',...
                'Rshoulder_flexion','Lshoulder_flexion','
                    Rshoulder_abduction','Lshoulder_abduction'
                    ,...
                'Relbow_flexion','Lelbow_flexion',...
                'xbodyCM',...
                'ybodyCM',...
                'zbodyCM',...
                'Rtoex','Rtoey','Rtoez','Ltoex','Ltoey','
                    Ltoez','Rheelx','Rheely','Rheelz','Lheelx'
                    ,'Lheely','Lheelz','RAJCx','RAJCz','LAJCx'
                    ,'LAJCz'};

%% Set file names for processing
%firstAnkle = 1; % put manually from event file
%find the file name after string splits
mFileNameArr = strsplit(jointAngleFile,'_');
sizeMFileName = size(mFileNameArr);
%Remove .txt from last cell
if sizeMFileName(2) == 6
    tempString = strsplit(mFileNameArr{6},'.');
else
    tempString = strsplit(mFileNameArr{5},'.');
end
%create string from Arr
if sizeMFileName(2) == 6
    mFileName = strcat(mFileNameArr{3},'_',mFileNameArr{4},'_
        ',mFileNameArr{5},'_',tempString{1});
else
    mFileName = strcat(mFileNameArr{3},'_',mFileNameArr{4},'_
        ',tempString{1});
end
%Split the list of files from excel variables
eventTextFileNames = [eventText(2:end,2)];
%compare selected file names to all the files names to get
    col
fileNameRow = find(strcmp(eventTextFileNames,mFileName));
%% Determine whether trial is a fall or recovery
%extract information from the excel file
if eventData(fileNameRow,7) == 1
    fallResult = 1;
else
    fallResult = 0;
```

```
end

%% Plot relevant data on the time scale
%This is the time scale plot of the ankle angle
freq = 1/250;
tVec = (0:1/250:((length(data)-1)*freq))'; %create the time
    vector with respect to the frequency of the capture
%Select Stepping ankle
%rightAnkle = 2, leftAnkle = 1
stepAnkle = eventData(fileNameRow,4); %extract information
    from the excel file
%Store values from event data
treadStart = eventData(fileNameRow,2);%extract information
    from the excel file
stepStart1 = eventData(fileNameRow,3);%extract information
    from the excel file
stepDown1 = eventData(fileNameRow,5);%extract information
    from the excel file
%plot relevant ankle flexion data
%This processes the data only for the first stepping leg. Its
     usually the
%dominant leg of the subject
%% Extract the relevant joints
% Ankle Data
if stepAnkle == 1
    dataCol1 = find(strcmp(column_headers,'Lankle_flexion'));
        %Lankle_flexion
    pAnkleFlexion = data(:,dataCol1);
else
    dataCol1 = find(strcmp(column_headers,'Rankle_flexion'));
        %Rankle_flexion
    pAnkleFlexion = data(:,dataCol1);
end
%Shank Data
if stepAnkle == 1
    dataCol2 = find(strcmp(column_headers,'Lshank_flexion'));
        %LShank_flexion
    pShankFlexion = data(:,dataCol2);
else
    dataCol2 = find(strcmp(column_headers,'Rshank_flexion'));
        %RShank_flexion
    pShankFlexion = data(:,dataCol2);
end
%Trunk Data
dataCol3 = find(strcmp(column_headers,'trunk_flexion'));%
    Trunk Flexion
trunkFlexion = data(:,dataCol3);
```

```
%Knee Data
if stepAnkle == 1
    dataCol4 = find(strcmp(column_headers,'Lknee_flexion'));
       %LKnee_flexion
    pKneeFlexion = data(:,dataCol4);
else
    dataCol4 = find(strcmp(column_headers,'Rknee_flexion'));
       %RKnee_flexion
    pKneeFlexion = data(:,dataCol4);
end

%Hip Data
if stepAnkle == 1
    dataCol5 = find(strcmp(column_headers,'Lhip_flexion')); %
       LHip_flexion
    pHipFlexion = data(:,dataCol5);
else
    dataCol5 = find(strcmp(column_headers,'Rhip_flexion')); %
       RHip_flexion
    pHipFlexion = data(:,dataCol5);
end

%% Plot the time series of the relvant joints
% Ankle
f1 = figure;
plot(tVec,data(:,dataCol1));
title('Ankle flexion of primary foot');
xlabel('Time in seconds');
ylabel('Ankle Flexion angle');
hold on;
plot([tVec(treadStart) tVec(treadStart)],[min(data(:,dataCol1
   )) max(data(:,dataCol1))],'r');
hold on;
plot([tVec(stepStart1) tVec(stepStart1)],[min(data(:,dataCol1
   )) max(data(:,dataCol1))],'g');
hold on;
plot([tVec(stepDown1) tVec(stepDown1)],[min(data(:,dataCol1))
    max(data(:,dataCol1))],'b');
legend('AnkleAngle','Tread Start', 'Step Start', 'Step Down'
   );
fallResultString = strcat('Fall = ',num2str(fallResult)); %
   annotate whether the person fell down
dim = [.2 .5 .3 .3];
% annotation('textbox',dim,'String',fallResultString,'
   FitBoxToText','on');
```

```
%Shank

f2 = figure;
plot(tVec,data(:,dataCol2));
title('Shank flexion of primary foot');
xlabel('Time in seconds');
ylabel('Shank Flexion angle');
hold on;
plot([tVec(treadStart) tVec(treadStart)],[min(data(:,dataCol2
    )) max(data(:,dataCol2))],'r');
hold on;
plot([tVec(stepStart1) tVec(stepStart1)],[min(data(:,dataCol2
    )) max(data(:,dataCol2))],'g');
hold on;
plot([tVec(stepDown1) tVec(stepDown1)],[min(data(:,dataCol2))
     max(data(:,dataCol2))],'b');
legend('ShankAngle','Tread Start', 'Step Start', 'Step Down'
    );
fallResultString = strcat('Fall = ',num2str(fallResult)); %
    annotate whether the person fell down
dim = [.2 .5 .3 .3];
% annotation('textbox',dim,'String',fallResultString,'
    FitBoxToText','on');

%Trunk

f3 = figure;
plot(tVec,data(:,dataCol3));
title('Trunk flexion of primary foot');
xlabel('Time in seconds');
ylabel('Trunk Flexion angle');
hold on;
plot([tVec(treadStart) tVec(treadStart)],[min(data(:,dataCol3
    )) max(data(:,dataCol3))],'r');
hold on;
plot([tVec(stepStart1) tVec(stepStart1)],[min(data(:,dataCol3
    )) max(data(:,dataCol3))],'g');
hold on;
plot([tVec(stepDown1) tVec(stepDown1)],[min(data(:,dataCol3))
     max(data(:,dataCol3))],'b');
legend('TrunkAngle','Tread Start', 'Step Start', 'Step Down'
    );
fallResultString = strcat('Fall = ',num2str(fallResult)); %
    annotate whether the person fell down
dim = [.2 .5 .3 .3];
% annotation('textbox',dim,'String',fallResultString,'
    FitBoxToText','on');
```

```
%Knee

f4 = figure;
plot(tVec,data(:,dataCol4));
title('Knee flexion of primary foot');
xlabel('Time in seconds');
ylabel('Knee Flexion angle');
hold on;
plot([tVec(treadStart) tVec(treadStart)],[min(data(:,dataCol4
    )) max(data(:,dataCol4))],'r');
hold on;
plot([tVec(stepStart1) tVec(stepStart1)],[min(data(:,dataCol4
    )) max(data(:,dataCol4))],'g');
hold on;
plot([tVec(stepDown1) tVec(stepDown1)],[min(data(:,dataCol4))
     max(data(:,dataCol4))],'b');
legend('KneeAngle','Tread Start', 'Step Start', 'Step Down')
    ;
fallResultString = strcat('Fall = ',num2str(fallResult)); %
    annotate whether the person fell down
dim = [.2 .5 .3 .3];
% annotation('textbox',dim,'String',fallResultString,'
    FitBoxToText','on');

%Hip

f5 = figure;
plot(tVec,data(:,dataCol5));
title('Hip flexion of primary foot');
xlabel('Time in seconds');
ylabel('Hip Flexion angle');
hold on;
plot([tVec(treadStart) tVec(treadStart)],[min(data(:,dataCol5
    )) max(data(:,dataCol5))],'r');
hold on;
plot([tVec(stepStart1) tVec(stepStart1)],[min(data(:,dataCol5
    )) max(data(:,dataCol5))],'g');
hold on;
plot([tVec(stepDown1) tVec(stepDown1)],[min(data(:,dataCol5))
     max(data(:,dataCol5))],'b');
legend('HipAngle','Tread Start', 'Step Start', 'Step Down');
fallResultString = strcat('Fall = ',num2str(fallResult)); %
    annotate whether the person fell down
dim = [.2 .5 .3 .3];
% annotation('textbox',dim,'String',fallResultString,'
    FitBoxToText','on');
```

```
%% Process second leg
%This is the processing for the second leg, uncomment if
    necessary. This
%might cause runtime errors.
% secondStep = eventData(fileNameRow,12);
%
% if secondStep ~= 0
%     stepStart2 = eventData(fileNameRow,12);
%     stepDown2 = eventData(fileNameRow,14);
% end
%
% if secondStep == 1
%     dataCol2 = find(strcmp(column_headers,'Lankle_flexion')
    );
%     sAnkleFlexion = data(:,dataCol1);
% elseif secondStep == 2
%     dataCol2 = find(strcmp(column_headers,'Rankle_flexion')
    );
%     sAnkleFlexion = data(:,dataCol1);
% end
% % Plot if activity exist in second leg
% if exist('dataCol2')
%     figure
%     plot(tVec,data(:,dataCol2));
%     title('Angle flexion of secondary foot');
%     xlabel('Time in seconds');
%     ylabel('Angle Flexion angle');
%     hold on;
%     plot([tVec(treadStart) tVec(treadStart)],[min(data(:,
    dataCol1)) max(data(:,dataCol1))],'r');
%     hold on;
%     plot([tVec(stepStart2) tVec(stepStart2)],[min(data(:,
    dataCol1)) max(data(:,dataCol1))],'g');
%     hold on;
%     plot([tVec(stepDown2) tVec(stepDown2)],[min(data(:,
    dataCol1)) max(data(:,dataCol1))],'b');
%     legend('AnkleAngkle','Tread Start', 'Step Start', '
    Step Down');
% end

%% Phase plot processing for primary leg

%find derivative of primary ankle for phase plot
dTime = diff(tVec); %difference of time vector (dt)

%Differentiation of Ankle
```

```
dPAnkle = diff(pAnkleFlexion);%difference of angle vector (
    dtheta)
dPAnkleAngle = dPAnkle./dTime;%derivative of the angle with
    respect to time (dtheta/dtime)

%Differentiation of Shank
dPShank = diff(pShankFlexion);%difference of angle vector (
    dtheta)
dPShankAngle = dPShank./dTime;%derivative of the angle with
    respect to time (dtheta/dtime)

%Differentiation of Trunk
dTrunk = diff(trunkFlexion);%difference of angle vector (
    dtheta)
dTrunkAngle = dTrunk./dTime;%derivative of the angle with
    respect to time (dtheta/dtime)

%Differentiation of Knee
dPKnee = diff(pKneeFlexion);%difference of angle vector (
    dtheta)
dPKneeAngle = dPKnee./dTime;%derivative of the angle with
    respect to time (dtheta/dtime)

%Differentiation of Hip
dPHip = diff(pHipFlexion);%difference of angle vector (dtheta
    )
dPHipAngle = dPHip./dTime;%derivative of the angle with
    respect to time (dtheta/dtime)

%plot phase plot from tread start to some time after step
    down
afterStepDown = stepDown1 + (stepStart1 - treadStart); %
    calculate the various duration of the plots(e.g. tread
    start - step start duration)
if afterStepDown > length(dPAnkleAngle)
    afterStepDown = length(dPAnkleAngle)
end



%% Plot Phase plots
%Ankle
f6 = figure;
plot(dPAnkleAngle(treadStart:stepStart1),pAnkleFlexion(
    treadStart:stepStart1),'b');
hold on;
plot(dPAnkleAngle(stepStart1:stepDown1),pAnkleFlexion(
```

```
    stepStart1:stepDown1),'r');
hold on;
plot(dPAnkleAngle(stepDown1:afterStepDown),pAnkleFlexion(
    stepDown1:afterStepDown),'g');
title('Phase plot for primary ankle angle');
xlabel('\theta of primary ankle');
ylabel('$\dot{\theta}$ of primary ankle','interpreter','latex
    ')
legend('TreadStart','StepStart','StepDown');

% Shank
f7 = figure;
plot(dPShankAngle(treadStart:stepStart1),pShankFlexion(
    treadStart:stepStart1),'b');
hold on;
plot(dPShankAngle(stepStart1:stepDown1),pShankFlexion(
    stepStart1:stepDown1),'r');
hold on;
plot(dPShankAngle(stepDown1:afterStepDown),pShankFlexion(
    stepDown1:afterStepDown),'g');
title('Phase plot for primary Shank angle');
xlabel('\theta of primary Shank');
ylabel('$\dot{\theta}$ of primary Shank','interpreter','latex
    ')
legend('TreadStart','StepStart','StepDown');

% Trunk
f8 = figure;
plot(dTrunkAngle(treadStart:stepStart1),trunkFlexion(
    treadStart:stepStart1),'b');
hold on;
plot(dTrunkAngle(stepStart1:stepDown1),trunkFlexion(
    stepStart1:stepDown1),'r');
hold on;
plot(dTrunkAngle(stepDown1:afterStepDown),trunkFlexion(
    stepDown1:afterStepDown),'g');
title('Phase plot for Trunk angle');
xlabel('\theta of primary Trunk');
ylabel('$\dot{\theta}$ of Trunk','interpreter','latex')
legend('TreadStart','StepStart','StepDown');

% Knee
f9 = figure;
plot(dPKneeAngle(treadStart:stepStart1),pKneeFlexion(
    treadStart:stepStart1),'b');
hold on;
plot(dPKneeAngle(stepStart1:stepDown1),pKneeFlexion(
```

```
    stepStart1:stepDown1),'r');
hold on;
plot(dPKneeAngle(stepDown1:afterStepDown),pKneeFlexion(
    stepDown1:afterStepDown),'g');
title('Phase plot for primary Knee angle');
xlabel('\theta of primary Knee');
ylabel('$\dot{\theta}$ of primary Knee','interpreter','latex'
    )
legend('TreadStart','StepStart','StepDown');

% Hip
f10 = figure;
plot(dPHipAngle(treadStart:stepStart1),pHipFlexion(treadStart
    :stepStart1),'b');
hold on;
plot(dPHipAngle(stepStart1:stepDown1),pHipFlexion(stepStart1:
    stepDown1),'r');
hold on;
plot(dPHipAngle(stepDown1:afterStepDown),pHipFlexion(
    stepDown1:afterStepDown),'g');
title('Phase plot for primary Hip angle');
xlabel('\theta of primary Hip');
ylabel('$\dot{\theta}$ of primary Hip','interpreter','latex')
legend('TreadStart','StepStart','StepDown');
% Curve fit data

%% Ankle
choppedPAnkleAngle = pAnkleFlexion(treadStart:afterStepDown);
stepStartAnkle = choppedPAnkleAngle(stepStart1-treadStart);
stepStopAnkle = choppedPAnkleAngle(stepDown1-treadStart);
% [peakAnkle,peakAnkleTime] = max(choppedPAnkleAngle(
    stepStart1-treadStart:stepDown1-treadStart));
xChopped = [0:100/(afterStepDown-treadStart):100]';
fitAnkleModel = fit(xChopped,choppedPAnkleAngle,'
    smoothingspline');
xNew = 0:0.01:100;
fitPAnkleFlexion = fitAnkleModel(xNew);

%Derivative of Curvefit Data
dXNew = diff(xNew');
dFitPAnkleFlexion = diff(fitPAnkleFlexion);
dFitPAnkle = dFitPAnkleFlexion./dXNew;

%% Shank
choppedPShankAngle = pShankFlexion(treadStart:afterStepDown);
stepStartShank = choppedPShankAngle(stepStart1-treadStart);
stepStopShank = choppedPShankAngle(stepDown1-treadStart);
```

```
xChopped = [0:100/(afterStepDown-treadStart):100]';
fitPShankModel = fit(xChopped,choppedPShankAngle,'
    smoothingspline');
xNew = 0:0.01:100;
fitPShankFlexion = fitPShankModel(xNew);

%%Derivative of Curvefit Data
dXNew = diff(xNew');
dFitPShankFlexion = diff(fitPShankFlexion);
dFitPShank = dFitPShankFlexion./dXNew;

%% Trunk
choppedTrunkAngle = trunkFlexion(treadStart:afterStepDown);
stepStartTrunk = choppedTrunkAngle(stepStart1-treadStart);
stepStopTrunk = choppedTrunkAngle(stepDown1-treadStart);
xChopped = [0:100/(afterStepDown-treadStart):100]';
fitTrunkModel = fit(xChopped,choppedTrunkAngle,'
    smoothingspline');
xNew = 0:0.01:100;
fitTrunkFlexion = fitTrunkModel(xNew);

%%Derivative of Curvefit Data
dXNew = diff(xNew');
dFitTrunkFlexion = diff(fitTrunkFlexion);
dFitTrunk = dFitTrunkFlexion./dXNew;

%% Knee
choppedPKneeAngle = pKneeFlexion(treadStart:afterStepDown);
stepStartKnee = choppedPKneeAngle(stepStart1-treadStart);
stepStopKnee = choppedPKneeAngle(stepDown1-treadStart);
xChopped = [0:100/(afterStepDown-treadStart):100]';
fitPKneeModel = fit(xChopped,choppedPKneeAngle,'
    smoothingspline');
xNew = 0:0.01:100;
fitPKneeFlexion = fitPKneeModel(xNew);

%%Derivative of Curvefit Data
dXNew = diff(xNew');
dFitPKneeFlexion = diff(fitPKneeFlexion);
dFitPKnee = dFitPKneeFlexion./dXNew;

%% Hip
choppedPHipAngle = pHipFlexion(treadStart:afterStepDown);
stepStartHip = choppedPHipAngle(stepStart1-treadStart);
stepStopHip = choppedPHipAngle(stepDown1-treadStart);
xChopped = [0:100/(afterStepDown-treadStart):100]';
fitPHipModel = fit(xChopped,choppedPHipAngle,'smoothingspline
```

```
    ');
xNew = 0:0.01:100;
fitPHipFlexion = fitPHipModel(xNew);

%%Derivative of Curvefit Data
dXNew = diff(xNew');
dFitPHipFlexion = diff(fitPHipFlexion);
dFitPHip = dFitPHipFlexion./dXNew;

%% Save and Load data into the same .mat file
Ankle
try
    prevDataAnkleAngle = load(strcat(jointAngleFilePath,'
        AnkleProcessedData.mat'));
    pAnkleFlexionData = [prevDataAnkleAngle.pAnkleFlexionData
         fitPAnkleFlexion];
    save(strcat(jointAngleFilePath,'AnkleProcessedData.mat'),
        'pAnkleFlexionData');
catch
    pAnkleFlexionData = fitPAnkleFlexion;
    save(strcat(jointAngleFilePath,'AnkleProcessedData.mat'),
        'pAnkleFlexionData');
end

try
    prevDataDAnkleAngle = load(strcat(jointAngleFilePath,'
        DAnkleProcessedData.mat'));
    pDAnkleFlexionData = [prevDataDAnkleAngle.
        pDAnkleFlexionData dFitPAnkle];
    save(strcat(jointAngleFilePath,'DAnkleProcessedData.mat')
        ,'pDAnkleFlexionData');
catch
    pDAnkleFlexionData = dFitPAnkle;
    save(strcat(jointAngleFilePath,'DAnkleProcessedData.mat')
        ,'pDAnkleFlexionData');
end

%Shank
try
    prevDataShankAngle = load(strcat(jointAngleFilePath,'
        ShankProcessedData.mat'));
    pShankFlexionData = [prevDataShankAngle.pShankFlexionData
         fitPShankFlexion];
    save(strcat(jointAngleFilePath,'ShankProcessedData.mat'),
        'pShankFlexionData');
catch
    pShankFlexionData = fitPShankFlexion;
```

```
    save(strcat(jointAngleFilePath,'ShankProcessedData.mat'),
        'pShankFlexionData');
end

try
    prevDataDShankAngle = load(strcat(jointAngleFilePath,'
        DShankProcessedData.mat'));
    pDShankFlexionData = [prevDataDShankAngle.
        pDShankFlexionData dFitPShank];
    save(strcat(jointAngleFilePath,'DShankProcessedData.mat')
        ,'pDShankFlexionData');
catch
    pDShankFlexionData = dFitPShank;
    save(strcat(jointAngleFilePath,'DShankProcessedData.mat')
        ,'pDShankFlexionData');
end


%Trunk
try
    prevDataTrunkAngle = load(strcat(jointAngleFilePath,'
        TrunkProcessedData.mat'));
    pTrunkFlexionData = [prevDataTrunkAngle.pTrunkFlexionData
         fitTrunkFlexion];
    save(strcat(jointAngleFilePath,'TrunkProcessedData.mat'),
        'pTrunkFlexionData');
catch
    pTrunkFlexionData = fitTrunkFlexion;
    save(strcat(jointAngleFilePath,'TrunkProcessedData.mat'),
        'pTrunkFlexionData');
end

try
    prevDataDTrunkAngle = load(strcat(jointAngleFilePath,'
        DTrunkProcessedData.mat'));
    pDTrunkFlexionData = [prevDataDTrunkAngle.
        pDTrunkFlexionData dFitTrunk];
    save(strcat(jointAngleFilePath,'DTrunkProcessedData.mat')
        ,'pDTrunkFlexionData');
catch
    pDTrunkFlexionData = dFitTrunk;
    save(strcat(jointAngleFilePath,'DTrunkProcessedData.mat')
        ,'pDTrunkFlexionData');
end

%Knee
try
```

```
    prevDataKneeAngle = load(strcat(jointAngleFilePath,'
        KneeProcessedData.mat'));
    pKneeFlexionData = [prevDataKneeAngle.pKneeFlexionData
        fitPKneeFlexion];
    save(strcat(jointAngleFilePath,'KneeProcessedData.mat'),'
        pKneeFlexionData');
catch
    pKneeFlexionData = fitPKneeFlexion;
    save(strcat(jointAngleFilePath,'KneeProcessedData.mat'),'
        pKneeFlexionData');
end

try
    prevDataDKneeAngle = load(strcat(jointAngleFilePath,'
        DKneeProcessedData.mat'));
    pDKneeFlexionData = [prevDataDKneeAngle.pDKneeFlexionData
         dFitPKnee];
    save(strcat(jointAngleFilePath,'DKneeProcessedData.mat'),
        'pDKneeFlexionData');
catch
    pDKneeFlexionData = dFitPKnee;
    save(strcat(jointAngleFilePath,'DKneeProcessedData.mat'),
        'pDKneeFlexionData');
end

%Hip
try
    prevDataHipAngle = load(strcat(jointAngleFilePath,'
        HipProcessedData.mat'));
    pHipFlexionData = [prevDataHipAngle.pHipFlexionData
        fitPHipFlexion];
    save(strcat(jointAngleFilePath,'HipProcessedData.mat'),'
        pHipFlexionData');
catch
    pHipFlexionData = fitPHipFlexion;
    save(strcat(jointAngleFilePath,'HipProcessedData.mat'),'
        pHipFlexionData');
end

try
    prevDataDHipAngle = load(strcat(jointAngleFilePath,'
        DHipProcessedData.mat'));
    pDHipFlexionData = [prevDataDHipAngle.pDHipFlexionData
        dFitPHip];
    save(strcat(jointAngleFilePath,'DHipProcessedData.mat'),'
        pDHipFlexionData');
catch
```

```
    pDHipFlexionData = dFitPHip;
    save(strcat(jointAngleFilePath,'DHipProcessedData.mat'),'
        pDHipFlexionData');
end

%Save Fall Result

try
    prevDataFallResult = load(strcat(jointAngleFilePath,'
        FallResultData.mat'));
    fallResultData = [prevDataFallResult.fallResultData
        fallResult];
    save(strcat(jointAngleFilePath,'FallResultData.mat'),'
        fallResultData');
catch
    fallResultData = fallResult;
    save(strcat(jointAngleFilePath,'FallResultData.mat'),'
        fallResultData');
end

Save step Start/Stop

try
    prevDataStepStartInfo = load(strcat(jointAngleFilePath,'
        StepStartInfo.mat'));
    stepStartCollect = [stepStartAnkle;stepStartShank;
        stepStartTrunk;stepStartKnee;stepStartHip];
    stepStartInfo = [prevDataStepStartInfo.stepStartInfo
        stepStartCollect];
    save(strcat(jointAngleFilePath,'StepStartInfo.mat'),'
        stepStartInfo');
catch
    stepStartInfo = [stepStartAnkle;stepStartShank;
        stepStartTrunk;stepStartKnee;stepStartHip];
    save(strcat(jointAngleFilePath,'StepStartInfo.mat'),'
        stepStartInfo');
end
try
    prevDataStepStopInfo = load(strcat(jointAngleFilePath,'
        StepStopInfo.mat'));
    stepStopCollect = [stepStopAnkle;stepStopShank;
        stepStopTrunk;stepStopKnee;stepStopHip];
    stepStopInfo = [prevDataStepStopInfo.stepStopInfo
        stepStopCollect];
    save(strcat(jointAngleFilePath,'StepStopInfo.mat'),'
        stepStopInfo');
catch
```

```
    stepStopInfo = [stepStopAnkle;stepStopShank;stepStopTrunk
        ;stepStopKnee;stepStopHip];
    save(strcat(jointAngleFilePath,'StepStopInfo.mat'),'
        stepStopInfo');
end

%% Save Data to file
%This will save all the figures in your folder as jpg.
   Comment if not
%necessary
% figureName1 = strcat(jointAngleFilePath,mFileName,'_','
   timeSeries.jpg');
% saveas(f1,figureName1);
%
% figureName2 = strcat(jointAngleFilePath,mFileName,'_','
   phasePlot.jpg');
% saveas(f2,figureName2);

% if exist(strcat(jointAngleFilePath,'processedData.mat'))
%     prevData = load(strcat(jointAngleFilePath,'
   processedData.mat'));
%     prevAngleSize = length(prevData.ankleAnkleOut(:,end));
%     prevDAngleSize = length(prevData.dAnkleAngleOut);
%     if prevAngleSize >= length(pAnkleFlexion)
%         ankleAnkleOut = []
%     end
%
%     ankleAngleOut = [prevData.ankleAngleOut pAnkleFlexion];
%     dAnkleAngleOut = [prevData.dAnkleAngleOut dPAnkleAngle
   ];
%     treadStartOut = [prevData.treadStartOut treadStart];
%     stepStartOut = [prevData.stepStartOut stepStart1];
%     stepDownOut = [prevData.stepDownOut stepDown1];
%     save(strcat(jointAngleFilePath,'processedData.mat'),'
   ankleAngleOut','dAnkleAngleOut','treadStartOut','
   stepStartOut','stepDownOut');
% else
%     ankleAngleOut = pAnkleFlexion;
%     dAnkleAngleOut = dPAnkleAngle;
%     treadStartOut = treadStart;
%     stepStartOut = stepStart1;
%     stepDownOut = stepDown1;
%     save(strcat(jointAngleFilePath,'processedData.mat'),'
   ankleAngleOut','dAnkleAngleOut','treadStartOut','
   stepStartOut','stepDownOut');
% end
```